



# **REAL-TIME RECOMMENDATIONS FOR TRAFFIC CONTROL IN AN ITS SYSTEM DURING AN EMERGENCY EVACUATION**

**FINAL REPORT**

**SEPTEMBER 2021**

## **AUTHORS**

Lauren Davis, Xiuli Qu, Younho Seong  
North Carolina A&T State University (NCAT)

**US DEPARTMENT OF TRANSPORTATION GRANT 69A3551747125**



## **DISCLAIMER**

The contents of this report reflect the views of the authors, who are responsible for the facts and the accuracy of the information presented herein. This document is disseminated under the sponsorship of the Department of Transportation, University Transportation Centers Program, in the interest of information exchange. The U.S. Government assumes no liability for the contents or use thereof.

1. Report No.	2. Government Accession No.	3. Recipient's Catalog No.	
4. Title: Real-Time Recommendations for Traffic Control in an Intelligent Transportation System (ITS) During an Emergency Evacuation  Subtitle: Phase I Studies		5. Report Date December 2020	
		6. Source Organization Code	
7. Author(s) : Qu, Xiuli; Davis, Lauren; Seong, Younho; Meda, Harshitha; Mhatre, Sachin; Alabi, Miriam; Richmond, David		8. Source Organization Report No.  CATM-2021-R3-NCAT	
9. Performing Organization Name and Address  Center for Advanced Transportation Mobility Transportation Institute 1601 E. Market Street Greensboro, NC 27411		10. Work Unit No. (TRAIS)	
		11. Contract or Grant No. 69A3551747125	
12. Sponsoring Agency Name and Address  University Transportation Centers Program (RDT-30) Office of the Secretary of Transportation–Research U.S. Department of Transportation 1200 New Jersey Avenue, SE Washington, DC 20590-0001		13. Type of Report and Period Covered Final Report: May 2019 – December 2020	
		14. Sponsoring Agency Code USDOT/OST-R/CATM	
15. Supplementary Notes:			
16. Abstract  Recent hurricanes such as Irma (2017) and Florence (2018) caused mass evacuations and the issues occurring during the evacuations have been brought to the public attention. To address these issues, the project team has investigated significant cues for evacuation planners' decisions using a Linear Lens Model and machine learning algorithms, and has analyzed traffic data during hurricane evacuations in North Carolina to discover spatial-temporal evacuation traffic patterns and create predictive models of hurricane evacuation traffic volumes. Our results show that only one of the seven cues tested (wind speed) contributes to evacuation planners' decisions and the sensor locations at the same county and adjacent counties form the cluster for evacuation traffic prediction. These models and findings can support the deployment of an effective evacuation and improve the mobility of the people and evacuation resources during a hurricane. We have also proposed and tested the quantitative methods to quantify a hurricane disruption to the U.S. airport network and identify feasible airports to reroute disrupted flights. Our results show that the proposed methods can identify the airports to be disrupted by an approaching hurricane and feasible airports for flight rerouting, which can support airlines administrators to divert flights from the affected airports.			
17. Key Words  Hurricane Evacuation, Air Transportation, Road Transportation Networks, Evacuation Traffic Prediction, Decision Making, Rerouting, Resilience, Judgment Model, Machine Learning		18. Distribution Statement  Unrestricted; Document is available to the public through the National Technical Information Service; Springfield, VT.	
19. Security Classif. (of this report)  Unclassified	20. Security Classif. (of this page)  Unclassified	21. No. of Pages  80	22. Price  ...

## TABLE OF CONTENTS

TABLE OF CONTENTS.....	i
EXECUTIVE SUMMARY .....	1
DESCRIPTION OF PROBLEM.....	3
METHODOLOGY AND RESULTS .....	5
FINDINGS, CONCLUSIONS, RECOMMENDATIONS .....	38
REFERENCES .....	40
APPENDIX A: Data for the Judgment Model.....	43
APPENDIX B: Codes for Prediction Models of Hurricane Evacuation Traffic in Eastern North Carolina .....	46
APPENDIX C: Posters and Presentation Slides .....	53

## EXECUTIVE SUMMARY

In recent years natural disasters such as hurricanes, floods, and winter storms, have caused significant losses and disruptions to infrastructure, communities, and the economy. Effective preparation and quick response to natural disasters is very important for the mitigation of such losses and disruptions. As an important part of natural disaster preparation and response, evacuations often occur before or after a natural disaster. However, an effective evacuation involves complex planning, preparation and operations. Moreover, diverse human evacuation behavior, such as staying or evacuating from home, taking public transportation or driving private vehicles, and different times and routes to leave from the affected area, complicates the management of mass evacuations.

In the first phase of this CATM project, we investigated the components of North Carolina's Intelligent Transportation System (ITS), which include smart traffic signals, cameras, meters, and dynamic message signs, and then identified potential actions for traffic control of an ITS during a hurricane evacuation. We also investigated the most affected airlines at the most affected airport during Hurricane Matthew, and proposed and tested the quantitative methods to estimate the number of affected passengers during the hurricane, quantify a hurricane disruption to the U.S. airport network, and identify feasible airports to reroute flights from a disrupted airport. Our results showed that the topology of an airline's flight network may influence the number of flight passengers affected by a hurricane disruption, and that the proposed quantitative methods can identify the airports to be disrupted by an approaching hurricane and feasible airports for rerouting flights from the disrupted airports.

For hurricane evacuation, we requested and collected historical data related to hurricane evacuations from different sources. These data were used to discover spatial-temporal evacuation traffic patterns, predict the hourly traffic during the hurricane evacuation, and investigate significant cues for Evacuation Planners' decisions during a hurricane evacuation. Our analysis results showed that the traffic volume at a sensor location could be predicted by the traffic volumes at the sensor locations in the same county and adjacent counties, and revealed that the sensor locations at the same county and adjacent counties form the cluster, and the 25 sensor locations can be grouped into the four clusters.



Our results also showed that only one (wind speed) of the seven cues tested contributes to Evacuation Planners' decision.

The proposed graph theoretical and rerouting methods can support airports and airlines administrators to recognize the airports that might be affected by an approaching hurricane, and identify potential airports to divert flights from the affected airports. The predictive models created in our studies can be used to manage hurricane evacuations, including proper traffic control, estimating emergency responders needed, and preparing enough evacuation supplies such as gas, water, food, and hotel rooms. These models and findings will help emergency response agencies deploy effective evacuation operations and improve the mobility of the people and evacuation resources during a hurricane. Our results of the first phase of this CATM project have been published as three peer-reviewed conference papers and presented as posters and oral presentations at national professional conferences and regional transportation conferences and symposiums. One journal paper has been submitted. In addition, four graduate students (including one African American student and two female students) and two female undergraduate students (including one African American student) have been involved in this CATM project. The participation of these students can contribute to the diversity of the U.S. transportation workforce in the future.

## DESCRIPTION OF PROBLEM

As part of natural disaster preparation and response, evacuations often occur before or after natural disasters such as hurricanes and earthquakes. For example, nearly 7 million Florida residents evacuated from the state during Hurricane Irma (2017), making it the largest hurricane evacuation in the U.S. and causing significant traffic congestion and fuel shortage in Florida. Hurricane Irma also caused significant disruption to air transportation in Florida. Nearly 4000 flights were canceled according to one report by Flight Aware. In addition to canceling and diverting flights, airlines also added flights to get passengers out of the storm's path and moved their planes (some of which cost \$100 million) to other safe cities. United Airlines, Delta, and American added flights in advance of the hurricane to help get stranded passengers out of the storm's path. The storm's ripple effects were felt in other cities like Atlanta, where Delta canceled nearly 1000 flights, resulting in many passengers stranded at the airport. During Hurricane Florence (2018), evacuation orders were issued to 25 counties in North Carolina and South Carolina, causing approximately 1 million Carolinians to evacuate from their homes. However, some residents chose to shelter in place despite mandatory evacuation issued in their counties. Traffic congestion and fuel shortages occurred in the eastern coastal areas in North Carolina even though the state government prepared for the evacuation by closing public schools and issuing evacuation orders 3 days before landfall, arranging evacuation paths, and providing evacuation guides. A worse issue was that some people could not evacuate due to the closure of a bridge when they chose to evacuate later. Therefore, it is obvious that effective and proper traffic control is crucial during a mass evacuation.

Recently, information and communication technologies (ICT) have been incorporated in the N.C. transportation infrastructure to build intelligent transportation systems (ITSs), which include smart actuated signals, dynamic message signs, the roadway weather information system, reversible lane systems, and the traveler information management system. These ITSs provide us with opportunities to improve the effectiveness and efficiency of emergency response. For example, smart traffic signals and the traffic coordination network enable emergency vehicles to respond to incidents rapidly. During natural disasters, ITSs can also play an important role in mass emergency evacuations. In this CATM project,



we aimed to develop and integrate ecological models for human evacuation behavior prediction and hurricane evacuation traffic control in intelligent transportation infrastructure. The ultimate goal is to create a human-centered intelligent traffic control recommendation system to support mass evacuations. The research questions of the first phase of our CATM project are:

- What factors and actions in the current NC ITSs should be considered when recommending an initial traffic control plan to prepare for a hurricane evacuation?
- What are significant factors or cues for evacuation planners to make hurricane evacuation decisions?
- How should effective policies be designed for airline carriers to minimize the number of passengers and planes stranded in the path of a hurricane, i.e., scheduling additional flights?
- How are evacuation traffic flows spatial-temporal associated, and how can the evacuation traffic volumes be predicted based on their spatial-temporal associations?

## **METHODOLOGY AND RESULTS**

In this CATM project, we conducted five studies addressing hurricane evacuation and weather-related flights recovery. Before we conducted these studies, we investigated the components of North Carolina's Intelligent Transportation System (ITS), and identified the potential actions that are supported by the smart components in the current N.C. road transportation system, and can be used to improve traffic control during a hurricane evacuation. We also requested and collected historical data related to hurricane evacuations from different sources to support our CATM studies. The methodology and results of our five studies in Phase 1 of this CATM project are described in detail in the following subsections.

### **Study 1 – Transportation Network Resilience in Charlotte, North Carolina for Day-to-Day Disruptions**

#### **1.1 Research Problem**

Daily disruptions to transportation systems are almost inevitable. These disruptions such as weather conditions, human errors, and/or technical failures, that occur on a daily basis, often cause delays and congestion to the transportation system, which ultimately result in the waste of fuel and time for each automotive commuter. Cities with large populations and high utilization of their transportation systems are vulnerable to such disruptions. For example, Charlotte, North Carolina, is a major city, ranking the 16th most populous city in the United States, having a population that is over 872,000 [1]. Being such a large city, it is the hub of major businesses, travel, and events, which often means that there is high utilization of its road network. In other words, there is a high volume of vehicles that travel through Charlotte's transportation system.

Transportation network disruptions can cause traffic congestion and delays. According to the 2019 Urban Mobility Report from Texas A&M Transportation Institute, it is estimated that an auto commuter in Charlotte was delayed 57 hours as well as consumed 22 gallons of excess fuel yearly due to congestion, resulting in a yearly congestion cost of \$1,269 per auto commuter [2]. For this reason, this study aimed to analyze the network connectivity and topology as well as the traffic volumes of the road transportation network of

Charlotte, NC, to quantify the resilience of the overall transportation network and to identify the road segments that are the most critical to the efficiency of the transportation network with respect to daily disruptions. In this study, two approaches, betweenness centrality and hierarchal cluster analysis, were used to identify critical road segments in Charlotte.

## **1.2 Methodology**

To identify critical road segments and examine the resiliency of the transportation network of Charlotte, we first define the scope of the transportation network. In this study, we focused on the U.S. interstates and highways since they are the most driven upon and have the highest traffic volume on average. The transportation network we define consists of U.S. interstates 85, 485, 77, 277, and U.S. highways 21, 29, and 74. The links in our defined network are the road segments, while the nodes are the exits or the intersection of two road segments. We also defined a set of starting nodes and ending nodes. The starting and ending nodes represent the most populated cities surrounding Charlotte, including Concord City, Gastonia, Huntersville and Indian Trail in North Carolina, and Rock Hill in South Carolina. We then collected and processed the data to compute the weighted edge betweenness centrality of each road segment, as well as to conduct a hierarchal cluster analysis. The results from this study can be used to make recommendations for strategic route planning, which could ultimately aid in the reduction of excess fuel consumption, delay, and congestion costs per auto commuter.

### ***1.2.1 Data Preparation and Processing***

In this study, Google Maps was used to determine the latitude and longitude of each intersection, which were later used to determine the distance of each road segment in the transportation network. After data regarding the intersections and links had been collected, Python 3.4 and the package, Networkx were utilized to compute the betweenness centrality for the links.

The AADT for 2018 was collected from the NCDOT's website, which was used as a variable in the hierarchal cluster analysis. Both variables, AADT and distance, were normalized to  $[0, 1]$  to reduce the influence of outliers and avoid that one variable is much

more dominant than the other. The variables were normalized using Equation (1). Note that the descriptive statistics and distributions of both variables can be seen in Section 1.3.

$$x_{norm}^i = \frac{x^i - x_{min}}{x_{max} - x_{min}} \quad (1)$$

### 1.2.2 Edge Betweenness Centrality Indicator

The weighted edge betweenness centrality algorithm is utilized to assess road resilience by identifying, topologically, vulnerable road segments and intersections in Charlotte's highway transportation network. Let  $G(V, E)$  represent the transportation network of interest, where  $V = \{v_1, v_2, \dots, v_i, s_1, s_2, \dots, s_n, t_1, t_2, \dots, t_m\}$  denotes the set of locations and intersections (nodes) and  $E = \{e_1, e_2, \dots, e_j\}$  represents the set of road segments (links) between each node. Each edge  $e_j$  is associated with a weight  $w_j > 0$ , which represents the traveling distance or time through the edge.

Given a transportation network  $G(V, E)$ , the weighted edge betweenness centrality algorithm computes the betweenness centrality for each road segment within the network using

$$C_B(e) = \sum_{s \in S, t \in T} \frac{\sigma(s, t|e)}{\sigma(s, t)}, \quad (2)$$

where  $s \in \{s_1, s_2, \dots, s_n\} \subset V$ ,  $t \in \{t_1, t_2, \dots, t_m\} \subset V$ ,  $\sigma(s, t)$  denotes the number of shortest paths from node  $s$  to node  $t$ , and  $\sigma(s, t|e)$  represents the number of the shortest paths from  $s$  to  $t$  including edge  $e$ . A shortest path from node  $s$  to node  $t$  is defined as a path from  $s$  to  $t$  with a minimum total weight of the edges in the path [3]. Using the edge betweenness centrality algorithm, a betweenness centrality value is computed for each road segment in the Charlotte transportation network. The road segments with the highest betweenness centrality values are the most critical to the overall topological structure of the network. Although there are other centrality indicators, such as degree centrality and closeness centrality, to consider, we chose edge betweenness centrality since it allows us to identify critical road segments such that the disruption (removal) of those road segments (links) to the transportation network could affect the fluidity of the traffic between many pairs of intersections through the shortest paths between them [4].

### 1.2.3 Hierarchical Cluster Analysis

A hierarchical cluster analysis was conducted using Python 3.4 to classify and identify critical road segments in the transportation network of Charlotte. The parameters used were the annual daily traffic for 2018 and the distance of each road segment (in miles). The dendrogram (Figure 1.1) was computed using the Euclidean distance formula. From the dendrogram, we conclude that the  $k$  value (number of clusters) should be 3.

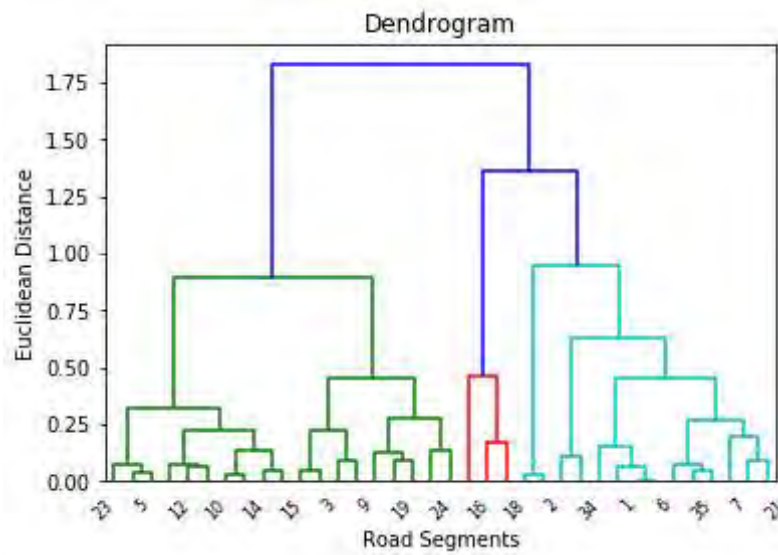


Figure 1.1: Dendrogram of road segments using Euclidean distance.

### 1.3 Results and Discussion

When exploring the data, we found that there were some extreme outliers in the average annual daily traffic (AADT) for 2018. Although the AADT and distance variables used contained extreme outliers, there were no erroneous values or inputs; the data occurred naturally given the dataset. Thus, none of the extreme outliers were dropped; however, both variables were normalized. The descriptive statistics of the AADT and the distance of each road segment are shown in Table 1.1. Figures 1.2 and 1.3 show the distribution of both variables, AADT, and distance.

Table 1.1: Descriptive statistics of the distances and average annual daily traffic for each road segment

Descriptive Statistics	Distance (miles)	AADT 2018
count	36	36
mean	4.386	100546
std	2.880	39155
min	0.4	15500
0.25	1.95	83604
0.5	3.9	99833
0.75	5.65	126786
max	12.1	174500

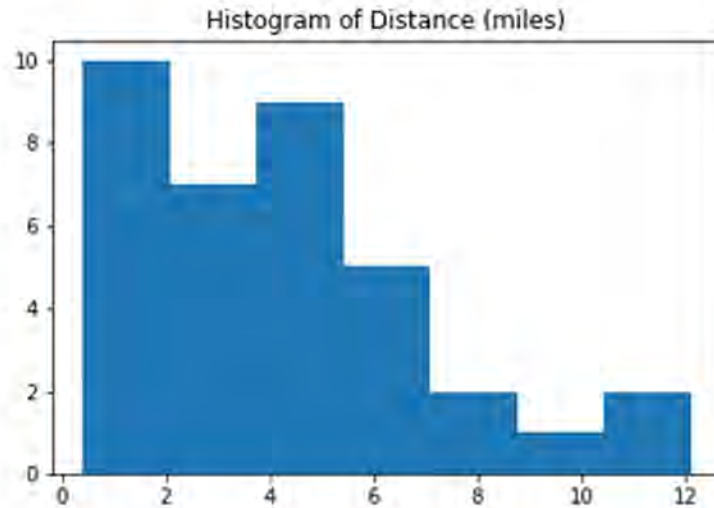


Figure 1.2: Histogram of the distances of each road segment.

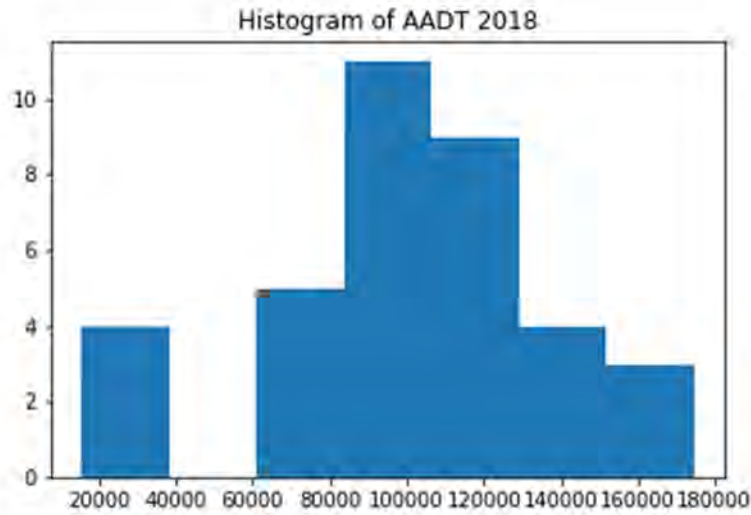


Figure 1.3: Histogram of the average annual daily traffic of each road segment.

After conducting the betweenness centrality analysis, we found that the road segments received a betweenness centrality value of either 0, 1, or 2. Figure 1.4 shows the transportation network with the betweenness centrality values colored as blue for 0, red for 1, and green for 2. The higher the betweenness centrality, the more critical the road segment to the entire transportation network.

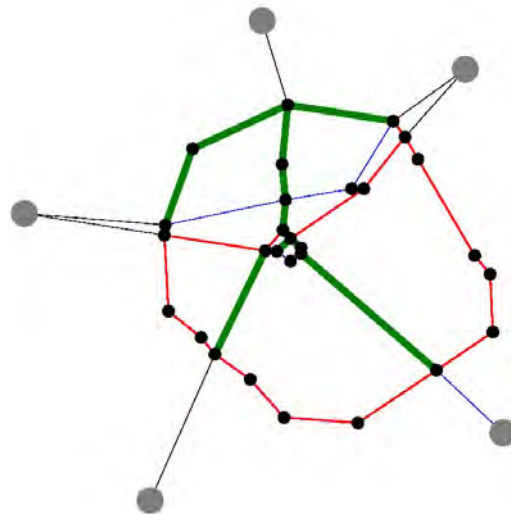


Figure 1.4: Charlotte highway segments grouped based on betweenness centrality.

To identify critical road segments, a hierarchical cluster analysis was conducted. After computing and examining the dendrogram, we allocated the observations to 3 different clusters, i.e., green, blue, and red clusters in Figure 1.5. In the figure, we notice that road segments that belong to the green cluster have the highest AADT, while those grouped in the red cluster, on average, have a lower AADT but a longer distance. On the other hand, the blue cluster contains road segments that have a higher AADT, on average, but a shorter distance. Figure 1.6 shows the transportation network considering the cluster groupings.

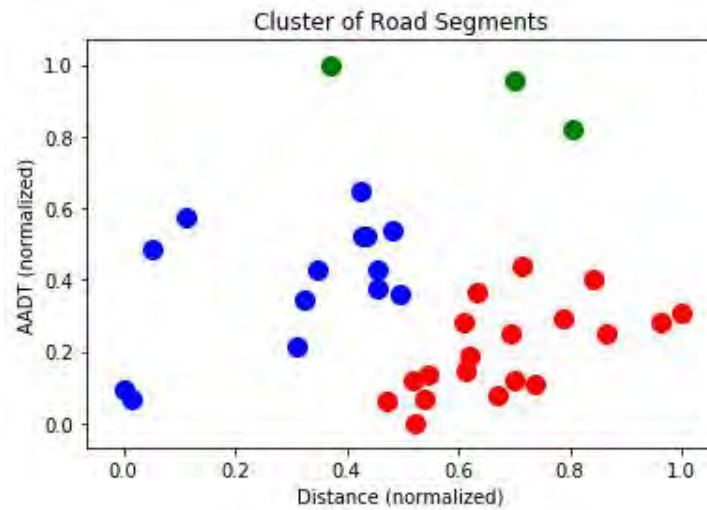


Figure 1.5: Clustering of road segments.

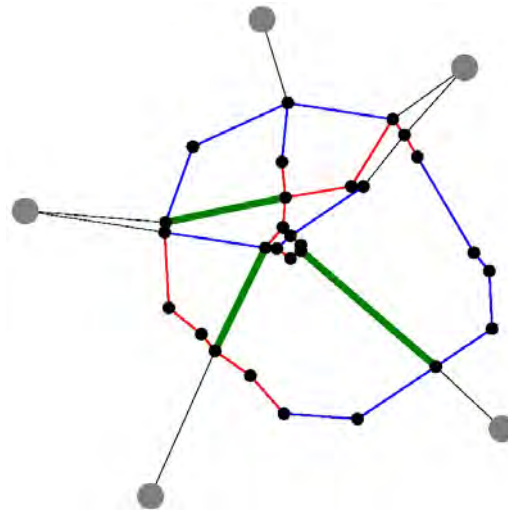


Figure 1.6: Charlotte highway segments clustered based on 2018 AADT.

Our results show that road segments of U.S. Interstates 485 and 77 and U.S. Highway 74 have the highest betweenness centrality value. This reveals that those are the most central links of the topological structure in the Charlotte highway transportation network. The disruption (removal) of the most critical links could affect the fluidity of the traffic through the shortest paths between many pairs of origins and destinations. Based on the hierarchical cluster analysis results, we conclude that the road segments belonging to the green cluster are the most critical since these road segments have the highest AADTs compared to the other road segments although they are not the longest road segments. This means that these road segments are more likely to be congested with an occurrence of disruption compared to the other road segments due to high traffic volume. The links that belong to the green cluster are road segments of U.S. Interstate 85 and 77 and U.S. Highway 74.

## **Study 2 – Data-Driven Approach to Estimate Airline Passengers Disruption**

### **2.1 Research Problem**

The United States (U.S.) airline companies serve millions of passengers and contribute to the country's economy in billions every year [5, 6]. To ensure passenger safety, convenience, and economic value, uninterrupted and efficient functioning of airline services is necessary. However, disruptions are not uncommon in an air transportation system, and disruption of any kind impacts planned flight schedules and can also lead to downstream effects. As per Bureau of Transportation Statistics (BTS) annual reports, more than 50% of disruptions in the aviation system are weather-related [5]. Hurricanes are one of the weather-related incidents that can significantly disrupt air travel due to their inclement nature. Moreover, some studies pointed out the fact that the network structure of air transportation or airlines might influence the general functionality of airlines operations [7]. During a disruption, different recovery actions could be implemented, and over the years, different planning and recovery tools or methods have been proposed [8-10]. Research on developing robust recovery methods and flight schedules may be essential for alleviating an airport system-related disruption. To achieve this, a prior step of appropriate data analysis of airport or airline big data might be influential in recommending certain actions during a disruption. In this study, we consider two-month flight data pertaining to four main airports in the southeast

region of the U.S. During the time frame considered in this dataset, Hurricane Matthew 2016 occurred. In this research, we set out to achieve the following research objectives:

1. To identify the most affected airlines and understand the influence of their network structure on the impact created during a hurricane disruption.
2. To estimate the possible number of impacted passengers during a hurricane disruption.

## 2.2 Methodology

The data used for this study was purchased from a leading provider of digital information called OAG [11]. The data set consists of 117,644 rows and 18 columns of information, for the period between September 1<sup>st</sup>, 2016 to October 31<sup>st</sup>, 2016. The scope of the data is limited to the departures and arrivals of four major airports in the Southeastern United States for all airline carriers. These airports are Orlando International Airport (MCO), Raleigh-Durham International Airport (RDU), Norfolk International Airport (ORF), and Ronald Reagan Washington National Airport (DCA). Hurricane Matthew was characterized as a post-tropical cyclone between September 28<sup>th</sup>, 2016 and October 9<sup>th</sup>, 2016. Hurricane Matthew in 2016 had its impact on states of Florida, Georgia, North Carolina, South Carolina, and certain parts of Virginia between October 7<sup>th</sup>, 2016 and October 9<sup>th</sup>, 2016 [12, 13]. Therefore, we selected this time period for our analysis. The data was filtered to remove rows with erroneous/empty information for further analysis (i.e., “NULL” values). We used the Networkx [14] package and other Python packages to conduct the data analysis.

Among the four airports present in our data set, we identified the most affected airport based on the change in their flight connections. The most affected airlines were recognized based on the summation of the count of flights for every airline for each selected day and affected airport. The network structure of the identified affected airlines was further analyzed to understand its impact on operations. To estimate the possible number of affected passengers, we have developed a set of mathematical equations. To conduct experiments with the developed equations, we have utilized the available number of seats in our dataset and load factors from the BTS website [15]. For the detailed version of our methods, please refer to our published work [16].

### 2.3 Results and Discussion

As per our analysis, during Hurricane Matthew, 2016, Orlando International Airport (MCO) was the most affected airport among the four airports present in the data set. MCO flight data was analyzed to understand different affected airlines. From Figure 2.1, we recognized the trend for every airline as the visualization shows the number of departure flights for each airline. As far as MCO departures are concerned, the most affected airlines in terms of the number of flights were American Airlines (AA), Delta Airlines (DL), Frontier Airlines (F9), JetBlue Airways (B6), Southwest Airlines (WN), Spirit Airlines (NK), and United Airlines (UA). Figures 2.2 – 2.8 show the network structures of these seven airlines constructed with the flight data present in the data set. Southwest was the most affected carrier with the highest number of flights canceled on October 6<sup>th</sup>, 7<sup>th</sup>, and 8<sup>th</sup> followed by JetBlue Airways. Spirit Airlines and Frontier Airlines were the least affected among the seven carriers. From examining the network topology and patterns of the seven affected airlines, most of them follow either a traditional hub-spoke model or focus city model except Southwest. Southwest Airlines follows a rolling hub model [17, 18]. However, further analysis of the network topology of Southwest along with other airlines is required for a stronger validation.



Figure 2.1: Departures at MCO before, during, and after the hurricane.

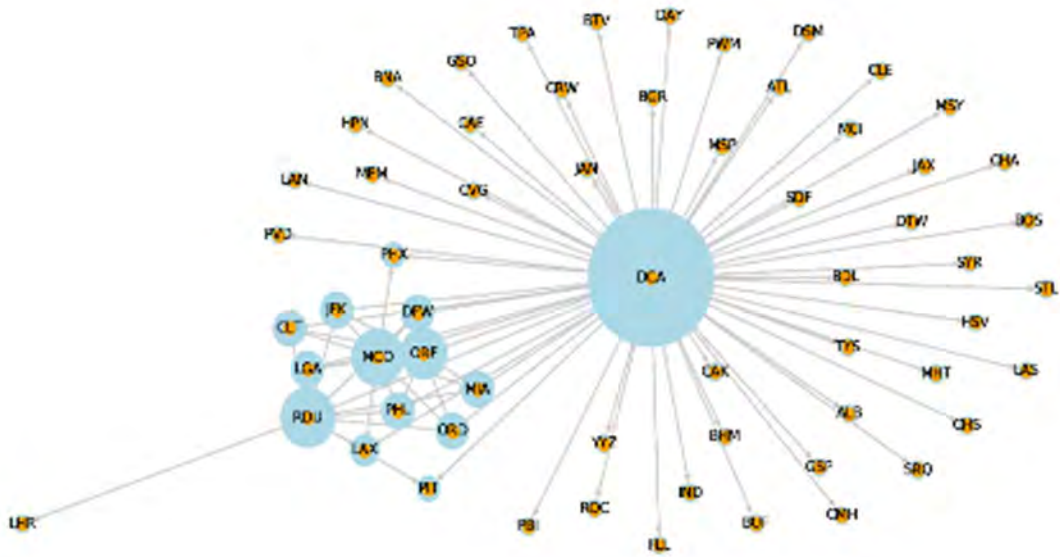


Figure 2.2: Network structure for American Airlines

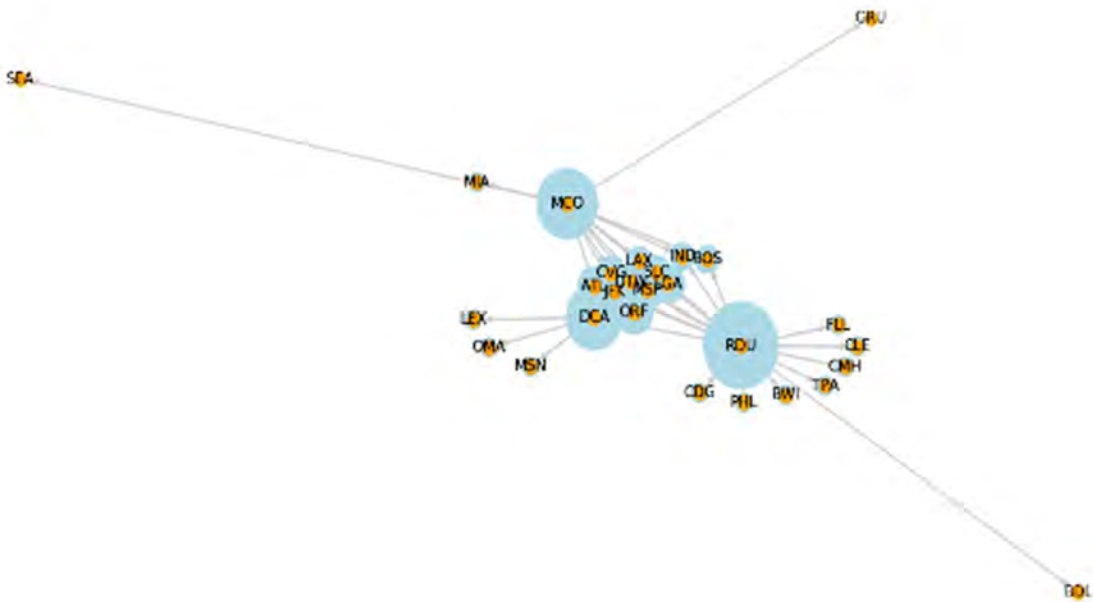


Figure 2.3: Network structure for Delta Airlines

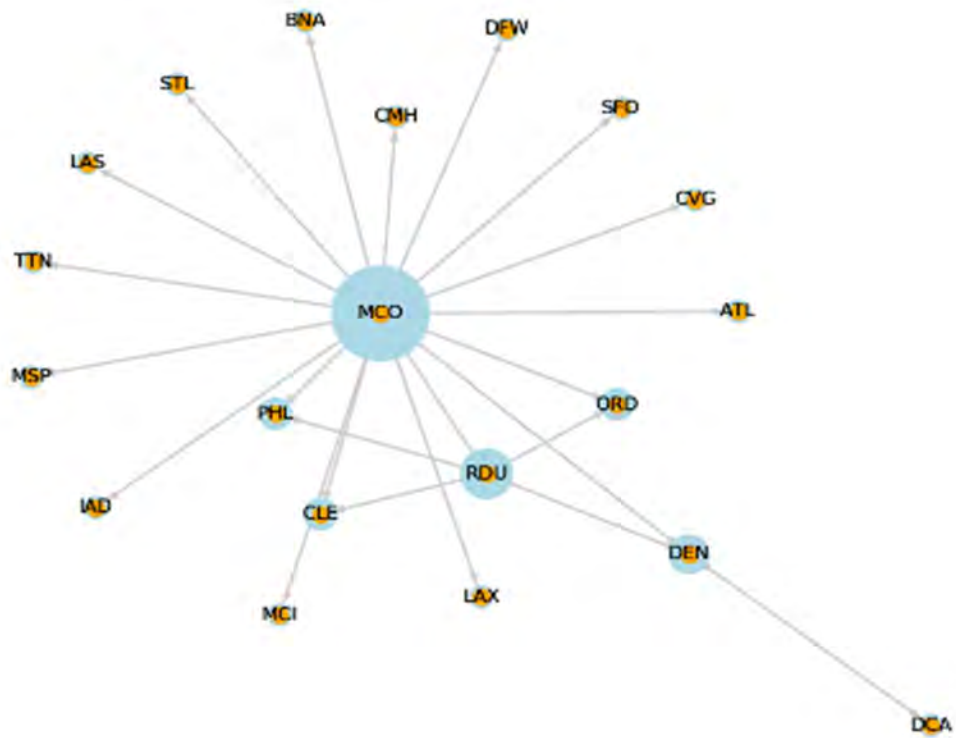


Figure 2.4: Network structure for Frontier Airlines

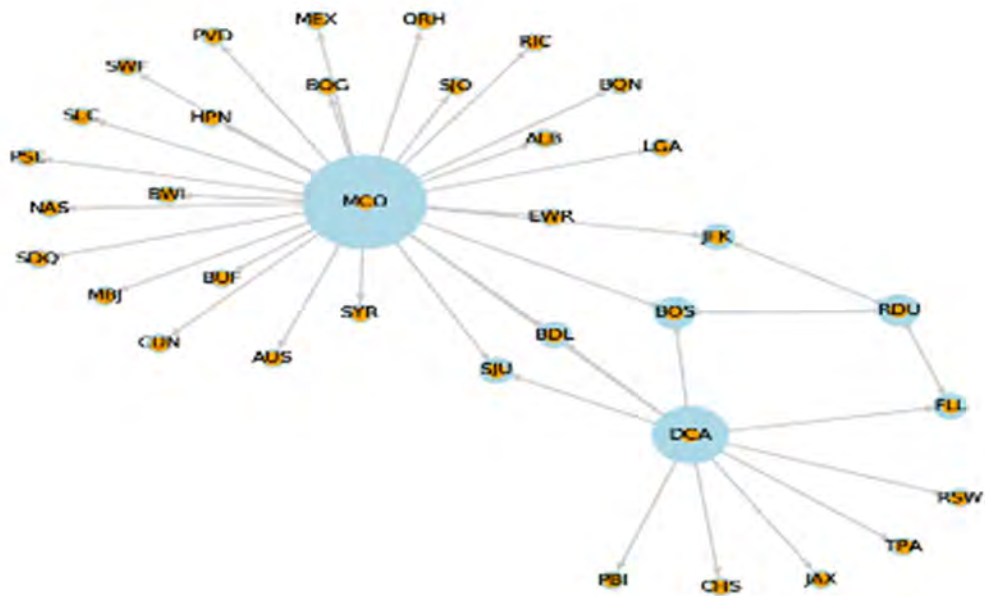


Figure 2.5: Network structure for JetBlue Airways

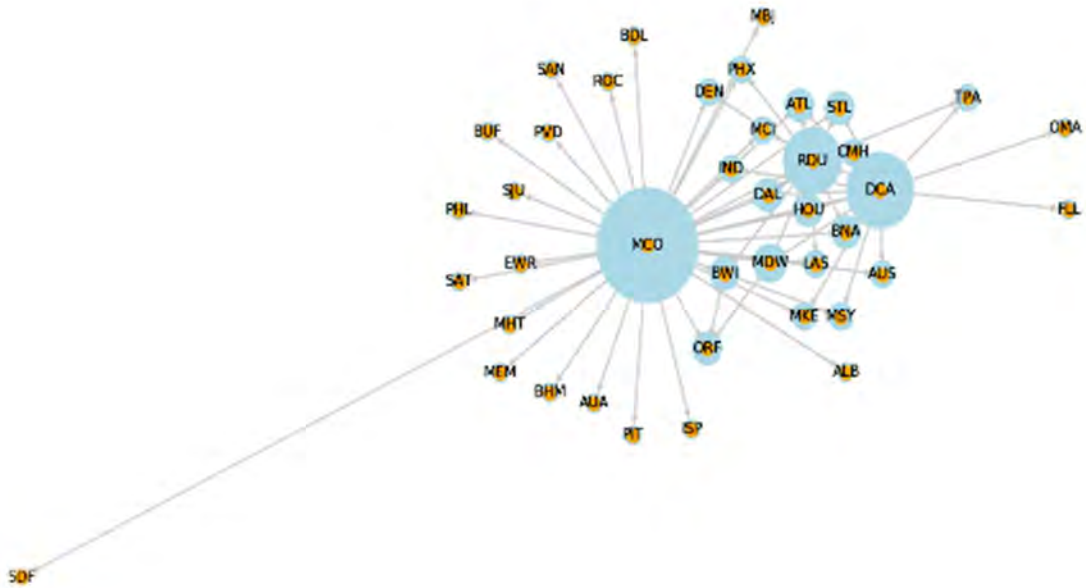


Figure 2.6: Network structure for Southwest Airlines

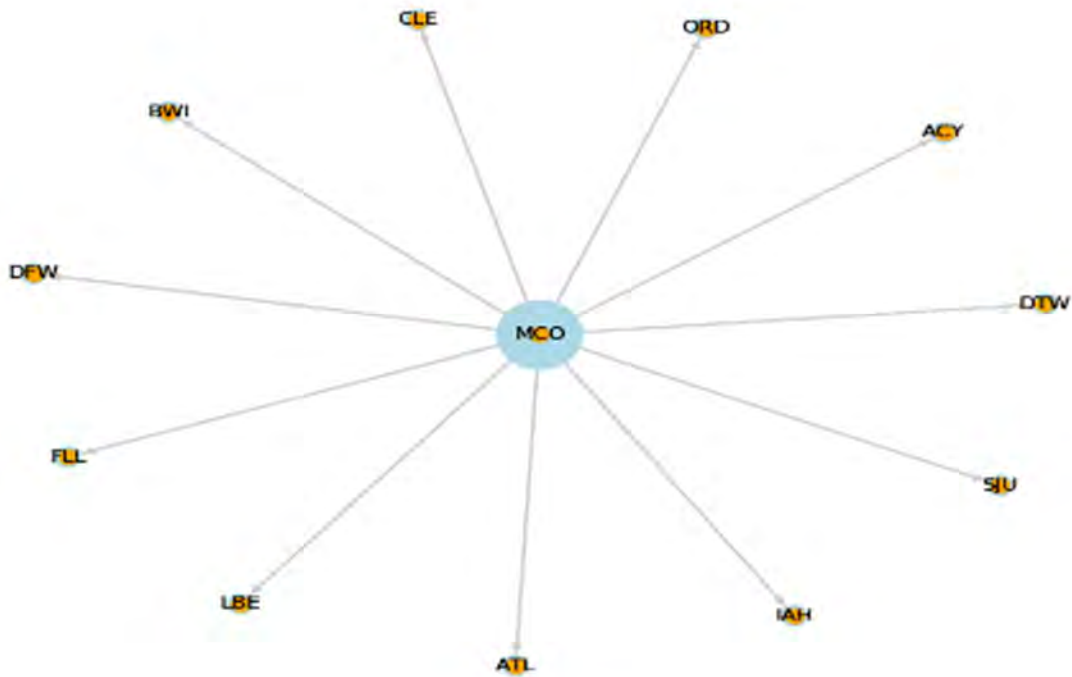


Figure 2.7: Network structure for Spirit Airlines

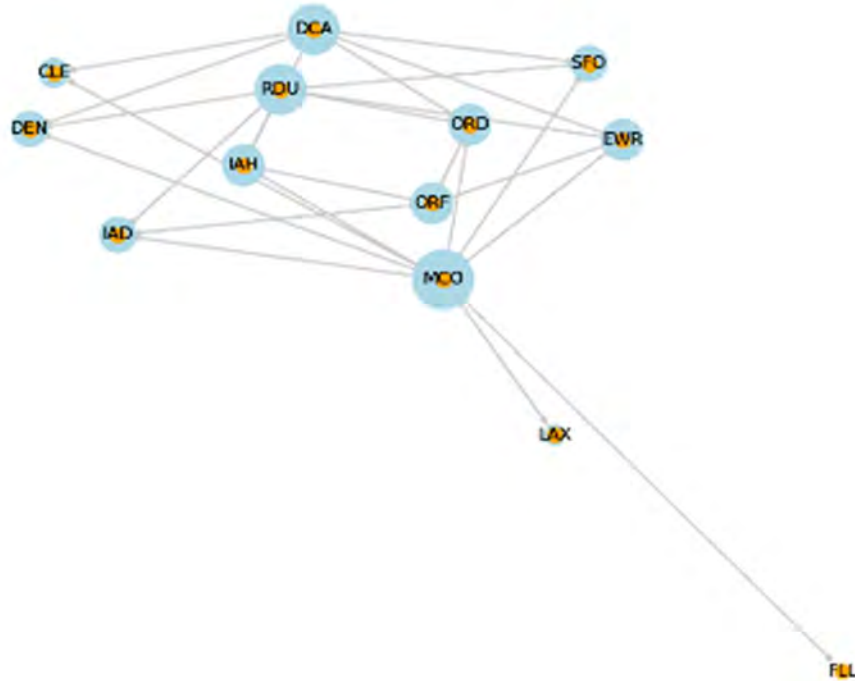


Figure 2.8: Network structure for United Airlines

Further, the predicted number of passengers for the seven affected airlines at MCO was determined. A comparison was made between these seven airlines based on the computation of the percentage of the predicted number of passengers. Figure 2.9 shows the percentage of the predicted number of affected passengers for departures of these seven airlines before, during, after the hurricane. The negative percentage value signifies the possible percentage of affected passengers for an airline carrier and excessively planned passengers if it is positive. From Figure 2.3, unlike other airlines, Southwest Airlines took almost two days to recover after the disruption at MCO caused by Hurricane Matthew. As MCO was completely closed on October 7<sup>th</sup>, 2016, it is evident that all the seven other carriers were affected only on this day.

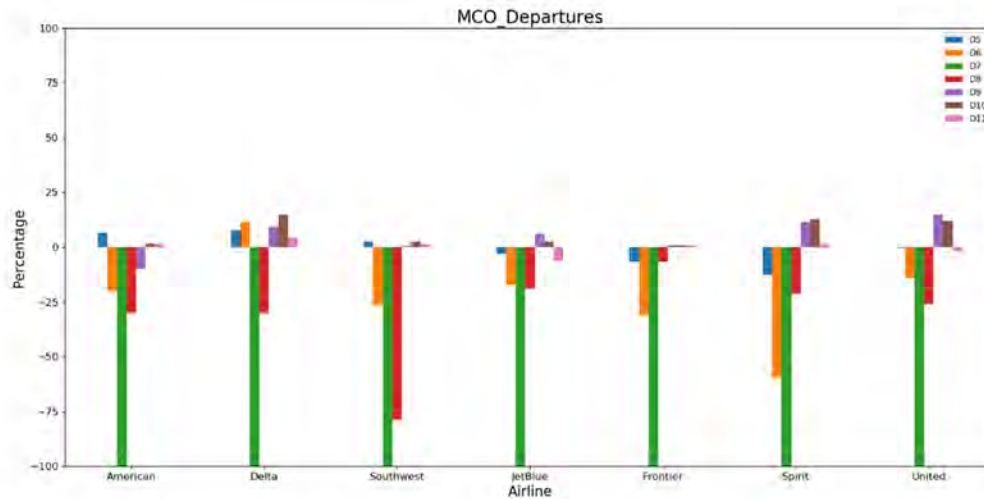


Figure 2.9: Percent of affected passengers for seven carrier airlines departures at MCO before, during, and after the hurricane.

From our analysis, we may relate the airline’s network topology with its possible number of affected passengers. However, extensive experimentation is required to develop and validate this relation. Moreover, the data-driven approach proposed in this study serves as a preliminary step to understand factors that influence passenger scheduling before, during, and after a disruption. In this study, we identified MCO to be the most affected airport and Southwest to be the most affected airline at this airport. Being aware of such information might aid in alleviating passenger disruption to a certain extent. As the data-driven approach does not discriminate the type of airport and kind of disruption, this methodology can also be extended to any other airport and disruption type.

### Study 3 – A Graph Theoretical Approach Integrating Geospatial Information to Analyze Airport Network Disruptions

#### 3.1 Research Problem

Disruptions in an air transportation system are not uncommon in occurrence, and especially weather-related ones are harder to predict and control due to their stochastic nature.

Hurricane and tropical storms are some of the weather-related disruptions that can lead to

significant economic impact along with root and propagated disruptions [19, 20]. In the past, a significant number of flights were canceled and delayed during certain hurricanes [21, 22]. The weather disruptions can also lead to significant delay costs, loss of passengers' goodwill, distorted operations and many more [23]. Due to the inclement and stochastic nature of certain weather-related events, it is not always possible to eliminate disruptions of this kind. However, locating airports in an airport network that might be impacted ahead of time may help in either planning or providing opportunities for recovery of a disruption. Additionally, there will be airports that will be affected due to these originally impacted airports. Therefore, capturing these two types of airports in an airport network might help in efficient planning, rescheduling, and recovery when a disruption occurs. Moreover, there might be a scenario where a flight path gets affected due to its proximity to a disrupted geographical zone. There are certain real-time situations where flights were diverted using different airports to avoid disruption or any adverse events, and it is essential to consider geography to include such scenarios [24, 25]. From our literature review, we have identified that geography consideration is absent when conducting airport network analysis related research [26-28]. In this study, we introduce this missing element as a geospatial scenario. Overall, we propose a graph theoretical method integrating geospatial elements to quantify airports from two different perspectives: disruptor and disruptee. A disruptor is an airport that gets impacted during a disruption along with flight routes connecting from or via this airport. A disruptee is an airport that is impacted by a disruptor. A pair of disruptor and disruptee is two airports where the latter is dependent on the former. In addition, we propose a rerouting method to discover feasible airports for rerouting from a disrupted airport.

### **3.2 Methodology**

In this study, we propose theoretical methods to quantify airports in an airport network from two different perspectives. In addition, we propose a rerouting method to identify feasible airports to reroute from a disrupted airport. To quantify the extent to which an airport is a disruptor, we propose a mathematical equation with three components: the immediate, the intermediate, and the geospatial components. The immediate component captures all immediate connections from an airport, whereas the intermediate component captures flight

routes for which an airport is an intermediate connection. The geospatial element captures flight routes that lie within a disrupted airport zone. The higher value of the disruptor equation indicates a highly disrupted airport and vice versa if it is a lower value.

To estimate the extent to which an airport could be a disruptee, we propose the disruptee equation. The disruptee equation consists of three components: the destination component, the transition component, and the geographical component. The destination component captures the number of flight paths originating from an airport that are affected due to a disruptor airport being their final destination. The transition component captures flight routes from an airport for which disruptor airports act as an intermediate connection. The geographical component estimates the flight paths from an airport that fall under the disrupted zone of the airport. Once the airports in an airport network are classified as disruptors and disruptees, rerouting passengers to different airports might aid in either avoiding or alleviating passenger disruption.

As a part of the rerouting method, we propose the rerouting metric that helps in identifying feasible airports for rerouting from a disrupted airport. It consists of three components: the change in disruptee equation value, the network proportion, and the airline network proportion. The change in disruptee equation value helps in quantifying an airport as either less or more disrupted than a disruptee. The network proportion helps in understanding if a similar set of destination airports are being operated from disruptee and rerouting airports. The airline network proportion indicates if the same airline companies are operating to the destinations from disruptee and rerouting airports.

To implement the proposed theoretical methods, we have constructed an airport network from world airlines routes data extracted from an open online source called “openflights.org”. The U.S. airport network constructed based on this data consisted of 2465 routes between 354 airports on 60 airlines. The hurricane forecast data available on National Hurricane Center is extracted to know storm location and time. For the detailed version of the proposed methodology and the data extraction process, please refer to the dissertation [29]. All the equations, methods, and analyses are developed as algorithms using Python programming [30].

### 3.3 Results and Discussion

To test the proposed methods, we have conducted a series of experiments considering hypothetical hurricane impact distance. We considered Fort Lauderdale/Hollywood International Airport (FLL) as a disruptor and 62 miles as a hurricane impact distance. With FLL as a disruptor, we have computed the disruptee equation values for remaining airports in an airport network. The top 20 disruptees with their respective component values are shown in Table 3.1. Though the destination and the transition component values are small for certain airports, they still appear as a top disruptee due to the geographical component value. This shows that there is a good chance of airports to be geographically impacted. The rerouting method was used to discover feasible airports within a distance of 50 miles for these top 20 disruptees. As a result, we have identified feasible airports for rerouting flights from each disruptee. The component values of the rerouting metric for the identified airports are as shown in Figure 3.1. Each airport is represented by its IATA code.

Table 3.1: Top 20 disruptees when FLL is a disruptor at a hurricane impact distance of 62 miles.

Airport (IATA code)	Destination Component	Transition Component	Geographical Component	Disruptee Equation Value	Airport Name
MIA	0.00000	0.02912	1.00000	0.50925	Miami International Airport, FL
PBI	0.00000	0.03196	1.00000	0.50275	Palm Beach International Airport, FL
ORH	0.50000	0.49150	0.03437	0.41035	Worcester Regional Airport, MA
IAG	0.20000	0.60032	0.03789	0.38100	Niagara Falls International Airport, NY
LBE	0.33333	0.42184	0.03073	0.33681	Arnold Palmer Regional Airport, PA
PBG	0.20000	0.38758	0.03908	0.28485	Plattsburgh International Airport, NY
EYW	0.12500	0.14984	0.29092	0.26624	Key West International Airport, FL
SWF	0.20000	0.24047	0.03509	0.21616	New York Stewart International Airport, NY
AVL	0.12500	0.17682	0.03611	0.15903	Asheville Regional Airport, NC
ISP	0.09091	0.13293	0.09280	0.15144	Long Island MacArthur Airport, NY
ACY	0.11111	0.13678	0.03450	0.13376	Atlantic City International Airport, NJ
HPN	0.06667	0.10938	0.07984	0.12382	Westchester County Airport, NY
LEX	0.07692	0.10731	0.03632	0.10619	Blue Grass Airport, KY
RIC	0.05556	0.07678	0.08405	0.10527	Richmond International Airport, VA
TTN	0.07692	0.10428	0.03480	0.10400	Trenton-Mercer Airport, NJ
GNV	0.00000	0.02736	0.19887	0.10283	Gainesville Regional Airport, FL
BDL	0.04348	0.06736	0.09290	0.09970	Bradley International Airport, CT
MYR	0.05000	0.09627	0.03527	0.08855	Myrtle Beach International Airport, SC
TYS	0.05882	0.08556	0.03567	0.08745	McGhee Tyson Airport, TN
JAX	0.04167	0.06560	0.07049	0.08707	Jacksonville International Airport, FL

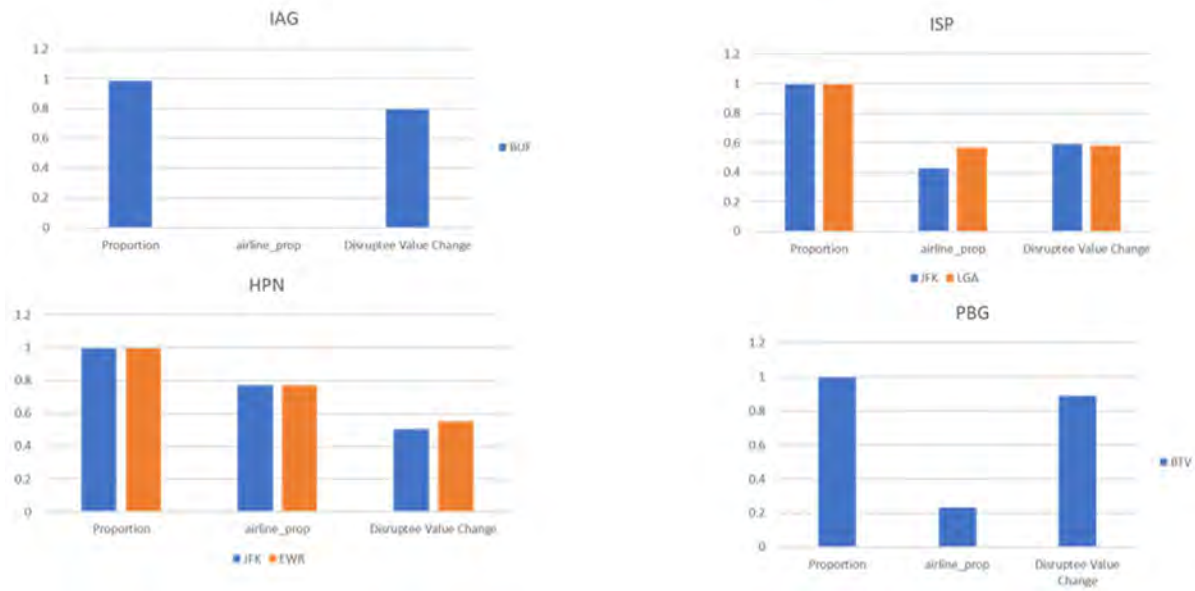


Figure 3.1: Rerouting airport choices within 50 miles radius for disruptees identified when FLL is a disruptor.

The airline network proportion value is zero for BUF airport when IAG is a disruptee. This shows that there are no common airline companies that operate to the destinations of BUF and IAG. The rerouting metric component values provide guidance in determining the most feasible airport when there are multiple choices for rerouting for certain disruptees. In Figure 3.1, ISP and HPN airports have multiple rerouting choices, whereas IAG and PBG airports have a single one.

Further experimentation revealed that ORD, DEN, and ATL are the top three disruptors in the U.S. airport network irrespective of the hurricane impact distance. Moreover, mostly large hub airports appeared as top 20 disruptors. Based on the adapted Hurricane Matthew, 2016 scenario, our results showed that the change in hurricane impact distance and forecast track do have an impact on identifying potential disruptors and their respective disruptees. This, in turn, impacted in discovering potential airports for rerouting. Please refer to the dissertation for detailed experimental results and findings [29].

## **Study 4 – Judgment Characterization for Emergency Evacuation Using Lens Model: A Machine Learning Approach**

### **4.1 Research Problem**

Intelligent Transportation Systems play an important role in mass emergency evacuations. In dealing with all humanitarian aspects of emergencies, emergency preparedness and disaster management are essential. Evacuation Planners (EP) and individuals' decisions during emergency preparation involve complex behavioral factors [31]. This study proposes to characterize EPs' decision-making behavior during emergency evacuation using machine learning algorithms and statistical methods. In doing so, a decision-making tool, the Brunswik Lens model, is used to describe the correlation between the environment and the behavior of organisms in the environment. Additionally, identifying significant cues for residents to decide dynamic evacuation routes under an uncertain environment and having incomplete information is somewhat limited due to how stochastic decision-making can be.

### **4.2 Methodology and Results**

In the modeling process, a judgment model is created with cues influencing the judgment. The researchers [32-34] considered the variables including wind speed, rainfall, number of households affected, flood level, median household income, and the poverty level. These variables (cues) were found to influence evacuation in North Carolina while preparing for an impending hurricane. The goal is to create a judgment model for an emergency to gain insight into the decision behavior of the various entities involved when the environment presents multiple cues.

The Judgment data about Hurricane Matthew was retrieved from multiple federal, state governments and other websites. All data collected are related to counties that were affected by Hurricane Matthew in the state of North Carolina. The weather-related data were collected from October 8<sup>th</sup> to 9<sup>th</sup>, 2016, when the hurricane approached. Socio-economic data such as poverty, median household income level, poverty level data, and disaster data were obtained for the year 2016 from the United States Census Bureau (USCB), United States Department of Agriculture Economic Research Service (USDA), and WebEOC [35], respectively. Weather data were mainly taken from National Oceanic and Atmospheric

Administration (NOAA) -and United States Geological Survey, respectively. The data collected consisted of seven variables and 42 observations (counties). All seven variables examined were numerical and were normally distributed.

#### 4.2.1 Brunswik Lens model

Figure 4.1 shows the Brunswik Linear Lens Model representation of single-system design (ecological criterion unavailable or not of interest) [36]. The Lens Model framework and its related parameters can capture and quantify judgment policies. Figure 4.1(a) represents the model of the criterion or environment. This model describes the relationship between the ecological criterion value (e.g., individuals' decision to evacuate or not) and the cue values accessible at the time a judgment is made. Figure 4.1(b) represents the judge's policy or strategy. It describes the relationship between the cue values and the criterion value. In Figure 4.1(b), the judgments are related to each cue, known as cue utilization validity. The pattern of cue utilization demonstrated by a judge determines the judgment policy,  $Y_S$ , represents the EPs' judgment and is modeled as a linear combination of a set of  $k$  cues ( $X_i, i = 1, \dots, k$ ).

$$Y_S = \sum_{i=1}^k \beta_{si} X_i + e \quad (3)$$

In Equation (3), the  $\beta_{si}$  denotes the weights of the cues that contribute to the judge's decision, and  $e$  represents the scope to which the cognitive model misses the actual value when trying to predict the judgment,  $Y_S$  [36]. Thus if  $\hat{Y}_S$  denotes the cognitive model, then

$$Y_S = \hat{Y}_S + e \quad (4)$$

The correlation between  $Y_S$  and  $\hat{Y}_S$  denoted by  $R_S$  measures the cognitive control with which a judgment strategy is executed. Consistency refers to the similarity between judgments made to repeated profiles of cue information [36].

$$R_S = \text{corr} (Y_S \hat{Y}_S) \quad (5)$$

#### 4.2.2 Machine learning algorithms

Supervised learning is a machine learning technique that uses computational learning theory, pattern recognition, and algorithm construction to map inputs to the output. Six (6) machine learning algorithms were also used to create the judgment model, namely linear discriminant

analysis (LDA), K-nearest neighbor (KNN), logistic regression (LR), classification and regression tree (CART), Naive-Bayes (NB), support vector machine (SVM). Python packages provide algorithms built in their libraries. Figure 4.2 shows the steps in Machine Learning.

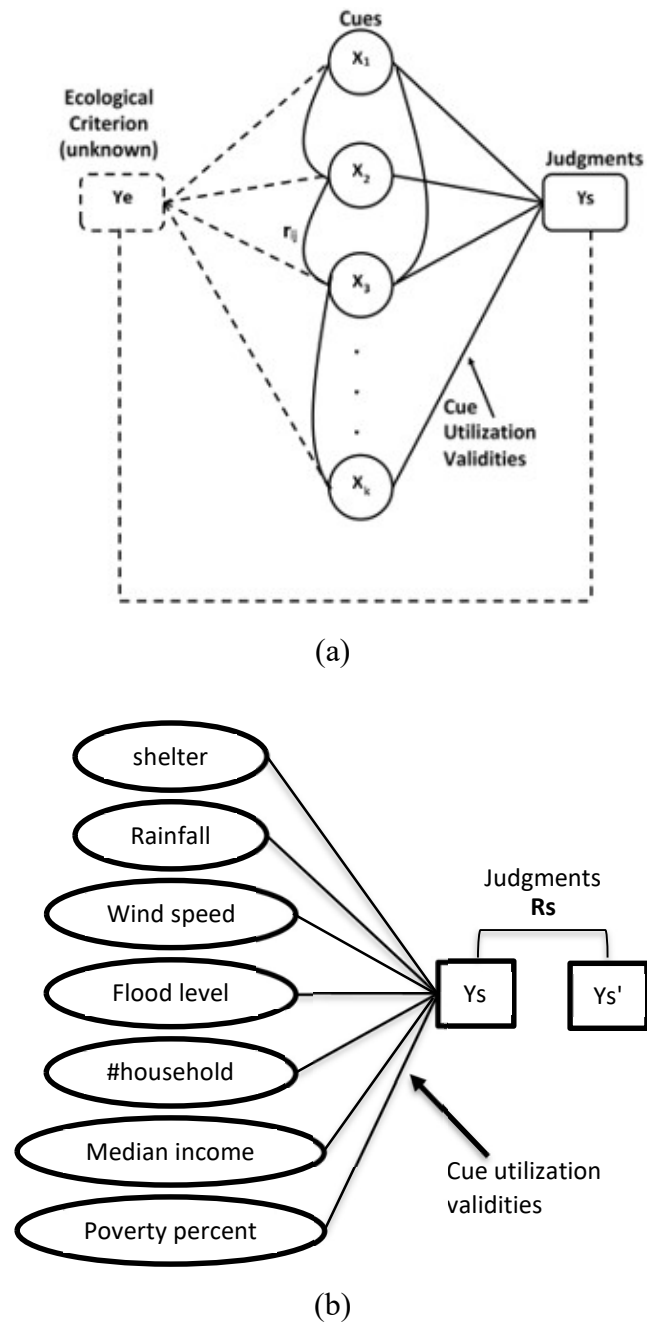


Figure 4.1: Brunswik Linear Lens Model representation of single system design (ecological criterion unavailable or not of interest).

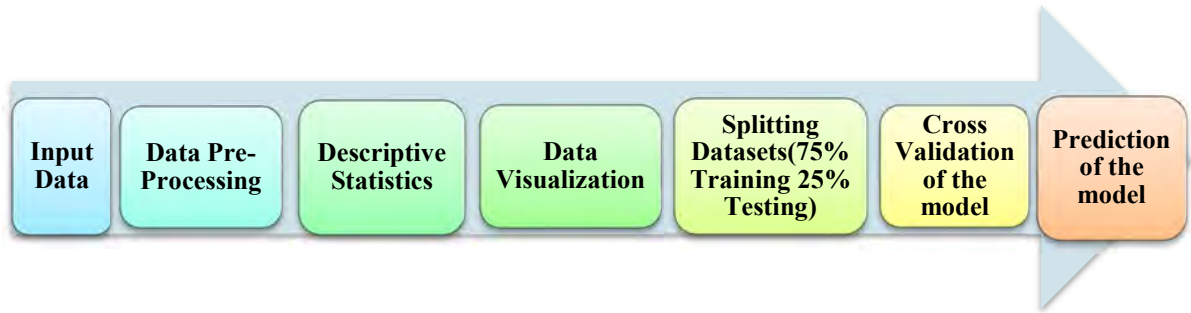


Figure 4.2: Steps in machine learning.

### 4.2.3 Evaluation metrics

The two performance metrics for the evaluation of models were Cross-Validation Accuracy (CVA) and Prediction/Model Accuracy (Accuracy). A 10-fold cross-validation is used in this study, and the accuracy is defined as:

$$Prediction\ Accuracy\ (PA) = \frac{TP+TN}{TP+TN+FP+FN} , \quad (6)$$

where  $TP$ ,  $TN$ ,  $FP$  and  $FN$  represent true positive, true negative, false positive, and false negative, respectively.

### 4.2.4 Lens model parameter, $(\hat{Y}_S)$ and $R_s$

The supervised machine learning techniques; LR, LDA, KNN, CART, NB, SVM as shown in Figure 4.3, also represented interesting accuracies but did not perfectly estimate the judgment model since model accuracies were 0.66, 0.72, 0.69, 0.6, 0.65 and 0.76, respectively. Figure 4.3 displays the cross-validation accuracy for all the machine learning models and data types after 75% of the judgment data is used in training them, and the model accuracy after 25% of the data is used to test the model. In the Judgment model, SVM generated a high CVA of approximately 73%, and LR, LDA and NB generated a PA of 72.7%.

The Lens model parameters are computed using the logistic regression for the judgment model. This technique is used as an idiographic-statistical approach to understanding the characteristics and conditions of individuals' behavior. This approach also helps to capture judgment policies as well as aspects of the judgment process. Logistic regression provides a statistical model that, in its basic form, uses a logistic function to model a dichotomous dependent variable.

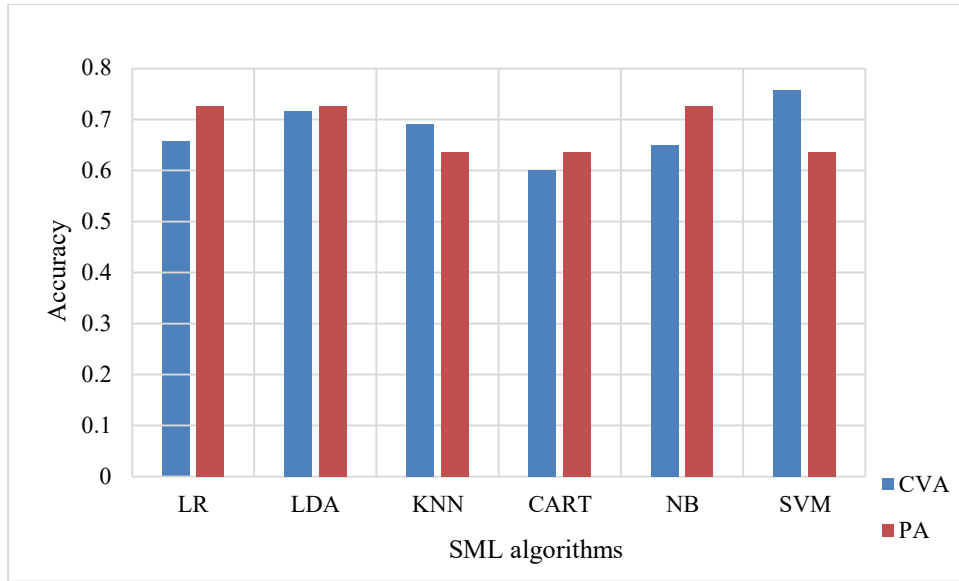


Figure 4.3: Accuracies of the six machine learning algorithms

### ***Dependent Variable***

In regression analysis, logistic regression (or logit regression) estimates the parameters of a logistic model (a form of binary regression). Mathematically, logistic regression estimates a multiple linear regression function defined as:

$$\text{logit}(p) = \log\left(\frac{p(y=1)}{1-(p=1)}\right) = \beta_0 + \beta_1 \cdot x_{12} + \beta_2 x_{12} + \dots \beta_p x_{in} \text{ for } i = 1, \dots, n. \quad (7)$$

In the selection of cues, backward elimination regression was used. In the backward elimination method, all the cues are initially used to build the model. Subsequently, the cue with the highest p-value is eliminated if the p-value is greater than the significance level (0.05). This is repeated, and a single cue is eliminated for each iteration until the cue shows a p-value less than 0.05. However, in this application, all the cues were eliminated except the wind speed. This means that only one of the cue weights contributed well enough to the model. The pseudo- $R^2$  value validates the performance of the model.

Figure 4.4 shows the results of logistic regression for judgment when all cues were used. Figure 4.4 shows the  $R^2$  for the judgment model ( $\hat{Y}_S$ ) and a correlation ( $r$ ) of 50.2%. For the judgment model ( $\hat{Y}_S$ ),  $R^2$  values were very low indicating that the cues were not able to produce the best model. Table 4.1 shows the weighting applied to each cue that

contributed to the EPs' judgment. These weights explain how the judge's policy was made based on the cue utilization validities.

Logit Regression Results						
=====						
Dep. Variable:	evacuate	No. Observations:	42			
Model:	Logit	Df Residuals:	34			
Method:	MLE	Df Model:	7			
Date:	Mon, 30 Nov 2020	Pseudo R-squ.:	0.2528			
Time:	19:21:34	Log-Likelihood:	-17.224			
converged:	True	LL-Null:	-23.053			
		LLR p-value:	0.1124			
=====						
	coef	std err	z	P> z	[0.025	0.975]
-----						
const	-1.5887	0.504	-3.150	0.002	-2.577	-0.600
Shelters	0.4428	0.590	0.751	0.453	-0.713	1.599
Wind_Speed	1.1022	0.526	2.096	0.036	0.072	2.133
Rainfall	-0.6706	0.595	-1.128	0.260	-1.836	0.495
Households	0.4337	0.538	0.806	0.420	-0.621	1.488
Flood_Lvl_ft	-0.0491	0.497	-0.099	0.921	-1.023	0.925
Median_Income	0.0962	0.813	0.118	0.906	-1.498	1.691
Poverty_Percent	0.2831	0.637	0.444	0.657	-0.966	1.532

Figure 4.4: Logistic regression output for judgment when all cues were used

Table 4.1: Cue weights

Cues	Relative(cue) weight
Shelters	0.144
Wind speed (mph)	0.358
Rainfall (in)	0.217
Households	0.141
Food level (ft)	0.016
Median Income (\$)	0.031
Poverty Percent (%)	0.092

### Independent variables

The total number of independent variables, also known as the cues in this context, is seven (7), as shown in Appendix A. Checking the correlation between the variables (cues) helps eliminate all redundant cues. The correlation between two variables is defined as:

$$r_{xy} = \frac{\sum(X_i - \bar{X})(y_i - \bar{y})}{\sqrt{\sum(X_i - \bar{X})^2 \sum(y_i - \bar{y})^2}}, \quad (8)$$

where

- $r_{xy}$  the correlation coefficient of the linear relationship between the variables  $x$  and  $y$
- $X_i$  – the values of the  $x$ -variable in a sample
- $\bar{X}$  – the mean of the values of the  $x$ -variable
- $y_i$  – the values of the  $y$ -variable in a sample
- $\bar{y}$  – the mean of the values of the  $y$ -variable

There were no high positive correlations among cues, as shown in Figure 4.5, indicating that all cues are independent and can be used for the prediction

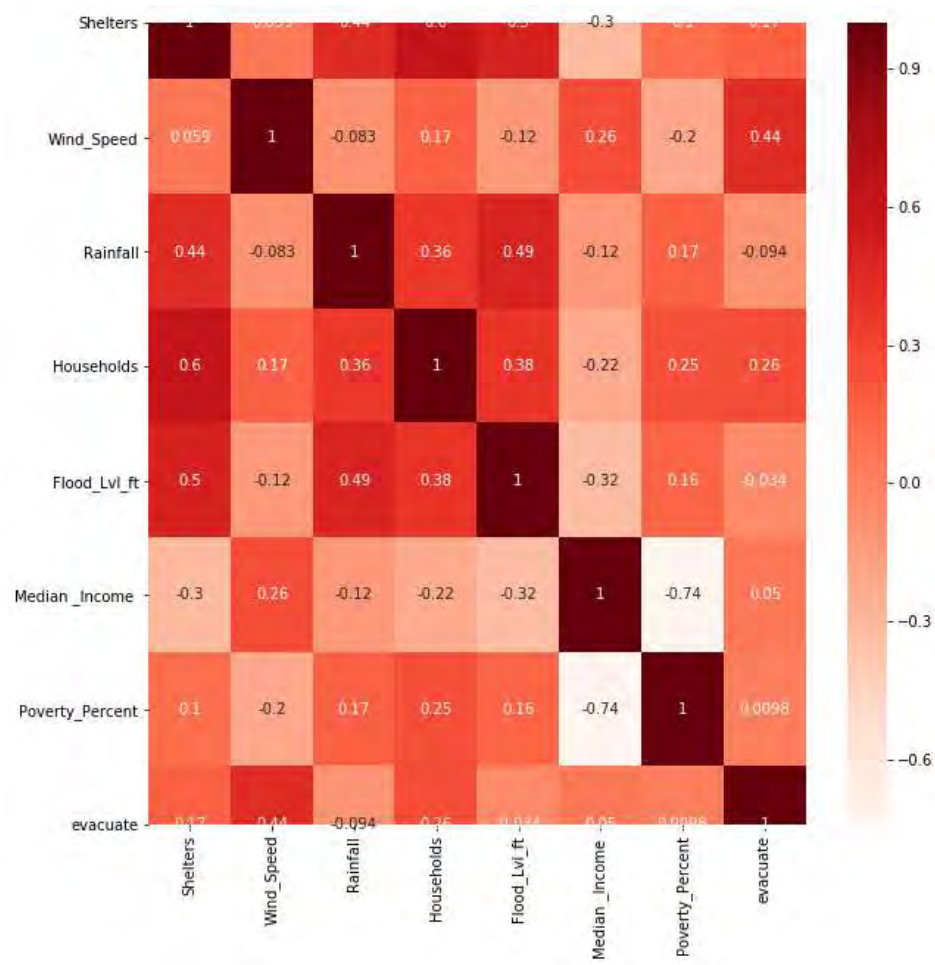


Figure 4.5: Correlation matrix for the cues

## **Study 5 – Visualization and Prediction Models of Hurricane Evacuation Traffic in Eastern North Carolina**

### **5.1 Research Problem**

Natural disasters affect millions of people, communities, and critical infrastructures every year in the world. According to the Center for Research on Epidemiology of Disaster (CRED), in 2019, there were 396 climate-related and geophysical disaster events recorded in the International Disaster Database (EM-DAT) with 11,755 deaths and over 95 million people affected across the world [37]. Over the last decade, the number and intensity of natural disasters, especially hurricanes, concerning the U.S. east coast have increased notably. According to the statistics, on average, 20 Hurricanes and eight floods have affected the United States every year since 2007. Many of them caused significant disruptions and losses to the communities, infrastructure, and economy. For example, recent hurricanes such as Matthew (2016), Harvey (2017), Irma (2017), Florence (2018), Michael (2018), Dorian (2019) affected the U.S. These hurricanes caused many casualties, damaged thousands of houses in the United States, and significantly disrupted critical infrastructures in the East Coast and Gulf Coast areas. These hurricanes also caused mass evacuations, in which millions of people traveled from the affected areas to safe locations before the landfalls.

Over the years, government agencies have guided millions of people for hurricane evacuation through road transportation systems in the best possible way. Similarly, in response to an approaching hurricane in North Carolina (N.C.), the government agencies, specifically disaster management agency which activates during the forecast of any hurricane, need to plan and carry out many preparation activities. One of the critical preparation activities is to plan and manage an effective evacuation in the potentially affected regions. Proper traffic control, sufficient emergency responders, and enough evacuation supplies such as gas, water, food, and hotel rooms are crucial for an effective mass evacuation. To decide traffic control policies and predict resources needed during a hurricane evacuation, the first step is to estimate the evacuation traffic volume and pattern when a hurricane approaches. To meet this need, in this study, we analyzed traffic flow data during Hurricane Florence evacuation in N.C. to discover space-time evacuation traffic patterns. Hourly traffic flow data during the hurricane evacuations were collected and provided by the

Departments of Transportation (DOTs) of North Carolina. Besides, we investigated the association of sensor locations to predict the hourly traffic during a hurricane evacuation.

## 5.2 Methodology

The primary sources of the data for this study are traffic counts from the traffic survey group of the NC Department of Transportation (NCDOT). The counties in N.C. are divided into fourteen DOT divisions, each division covering a group of the counties [38]. These divisions are also referred to as districts. The districts are allotted numbers starting from the eastern coast to western mountain regions. We requested the six coastal districts' traffic volume data for Hurricane Florence and Hurricane Dorian. The data sets cover traffic volume one week before hurricane landfall, one week during hurricane landfall, and one week after the hurricane landfall. In the current study, we analyzed the Hurricane Florence (2018) traffic volume data during a hurricane evacuation, i.e., five days before the hurricane landfall at the N.C. coastline. The traffic volume data of six coastal districts cover 42 counties in eastern North Carolina. The data was provided for thirty-eight sensor locations, consisting of one EXCEL file for each sensor location. Each EXCEL file contains the sensor location county, route number, lane direction, district number, and hourly traffic volume data with dates. Figure 5.1 illustrates the locations of some sensors on the different routes in North Carolina.

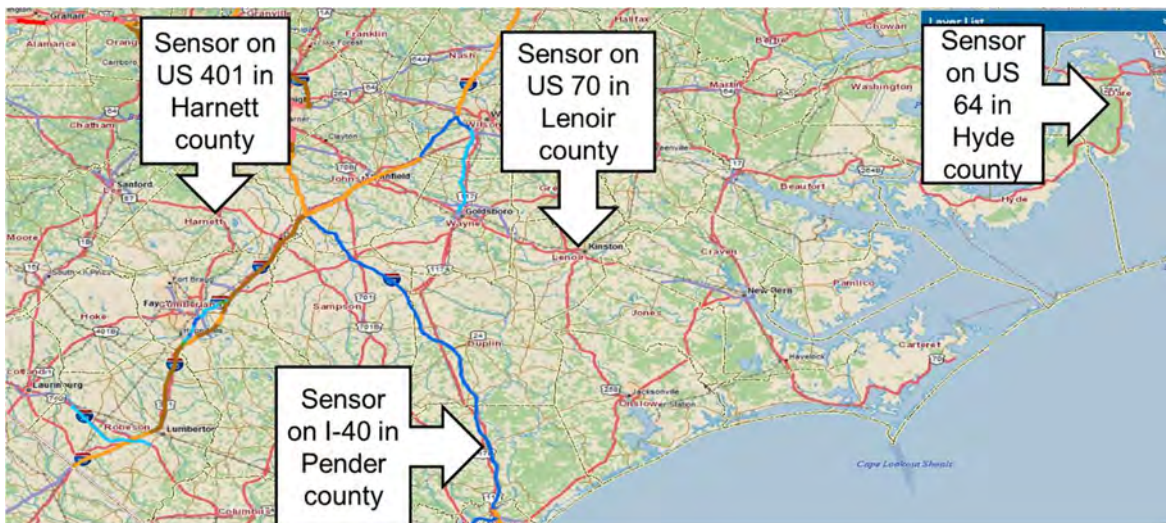


Figure 5.1: Illustration of different sensor locations in North Carolina.

Predictive modeling was used in this study to explore and analyze the traffic count data, infer the information about the traffic volume at each sensor location, and discover the sensor association. The collection and preparation of the input data required for the predictive analysis is a crucial step in the analysis. The input data for the predictive analysis was retrieved from the traffic count data received from NCDOT. Original data we obtained is separated by districts for each hurricane in the EXCEL sheets. For the predictive analysis, input data was prepared using different data exploration and data cleaning techniques in Python. After preparing the input data for the investigation, the data analysis is performed using the steps described in Figure 5.3. After analyzing the predictive analysis results, the sensor association was analyzed. Figure 5.2 depicts the overall methodology of the study.

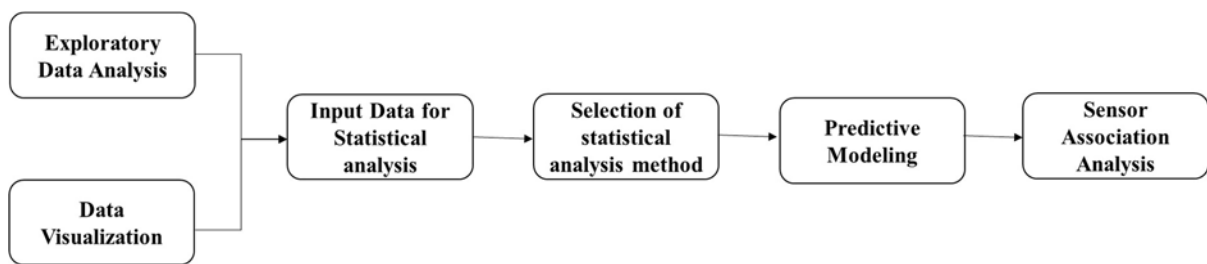


Figure 5.2: The methodology of the study

The linear regression [39] was used for assessing the association of traffic among the sensors in the study. The dependent variable (DV) for the linear regression is hourly traffic volume at a sensor location. The independent variables (IVs) for the linear regression consist of traffic volumes at the sensor location before 1 hour, 2 hours, 3 hours, and 4 hours and at other adjacent sensor locations before 1 hour, 2 hours, 3 hours, and 4 hours. Within four hours, the coastal county population can reach the resource center located at the States capital Raleigh.

The procedure for the statistical analysis is presented in Figure 5.3. In the statistical analysis, after preparing the input data and cleaning the data by omitting the data with missing value, if there were more than five feature variables (IVs), then the feature selection step is performed. In feature selection, we used the “backward elimination” method to select the most significant features. As the name suggests, firstly we need to feed all the possible

features to the model. We check the model's performance then iteratively remove the least correlated feature one by one until the model's overall performance comes in an acceptable range. The metric used to evaluate the feature correlation is  $p$ -values. If the  $p$ -value of a feature is above 0.05, then the feature is removed; otherwise, it is kept in the model. After that, we fitted the linear regression model of the selected features to the data, and tested the normality of residuals using the Normal QQ-plot and three different normality tests. The three normality tests are the Shapiro-Wilk test, the D'Angostino and Pearson's test, and the Anderson-Darling test. If the model passed the three tests, we stopped and accepted the model; otherwise, we did the outlier detection analysis.

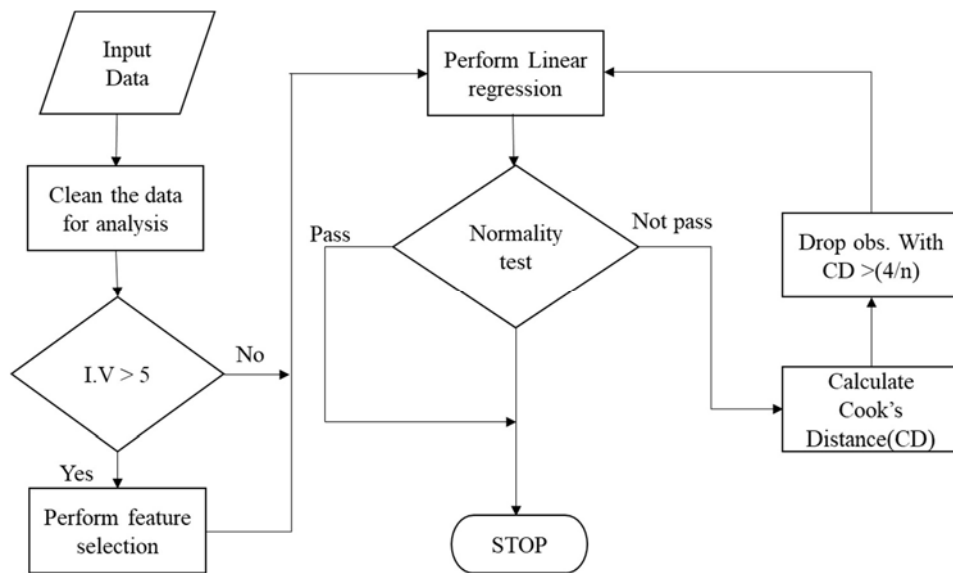


Figure 5.3: Procedure for statistical analysis.

In the outlier detection analysis, we calculate Cook's distance (CD) to identify the most influential observations in outlier detection. The observations with  $CD > (4/n)$  were dropped, where  $n$  is the total number of observations. After dropping the most influential observations, we fitted the model to the remaining data and tested the normality of residuals again. If the normality tests were passed, we stopped and accepted the model. Following the procedure, we fitted the regression models for the 25 selected sensor locations. Furthermore,

the regression models were used to study the traffic associations among the sensor locations, predicting the traffic volume at a sensor location during hurricane evacuation in the future.

### 5.3 Results and Discussion

Figure 5.4 graphically shows the traffic associations among the sensor locations based on the regression models for each location. In the graph, the node representing the sensor, and the arrow's direction represents the sensors' association. The incoming arrows to a sensor location show that the traffic at that sensor location is predicted from those incoming directed sensor locations. For example, the traffic volume at sensor A4201 is predicted by traffic volumes at sensor locations A2501, R9111, R9112, R9103, R9113, R9106, R9102, R9107, A5001D4, R5001, and previous traffic volumes at the same location A4201. Figure 4.1 reveals that the 25 locations can be grouped into the four clusters based on their traffic associations analytically and topologically.

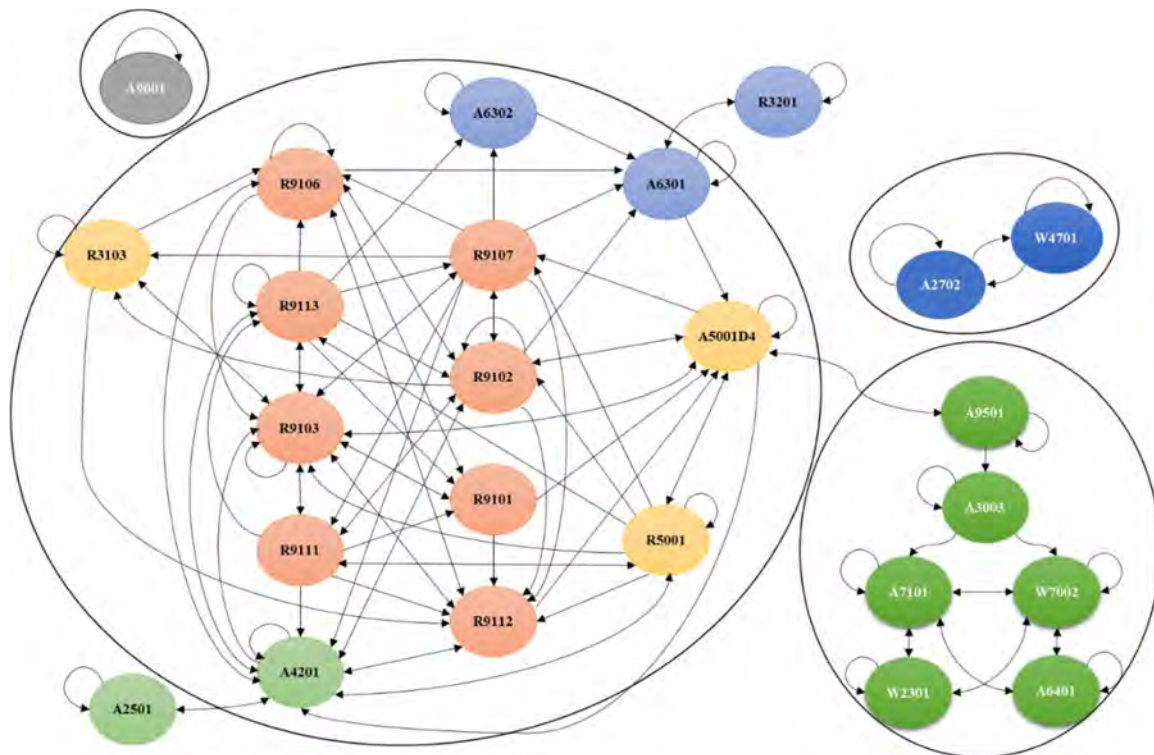


Figure 5.4: Sensor association in North Carolina for prediction of traffic volume during a hurricane evacuation.

Table 5.1: Sensor clusters and the counties they are located in

Sensor	County	Cluster
R9101	Wake	1
R9102	Wake	1
R9103	Wake	1
R9106	Wake	1
R9107	Wake	1
R9111	Wake	1
R9112	Wake	1
R9113	Wake	1
R5001	Johnston	1
A5001D4	Johnston	1
R3103	Durham	1
A4201	Harnett	1
A6301	Nash	1
A6302	Nash	1
A9501	Wayne	2
A3003	Duplin	2
A7101	Pender	2
W7002	Pender	2
A6401	New Hanover	2
W2301	Columbus	2
A2702	Dare	3
W4701	Hyde	3

Table 5.1. summarizes the sensor clusters and the county they are located in. Figure 5.1 and Table 5.1 reveal that the sensor locations from the same county and adjacent counties form the cluster, and the traffic volume at a sensor location can be predicted by the traffic volumes in the same county and adjacent counties. For example, sensors R9106, R9113, R9103, R9111, R9112, R9101, R9102, and R9107 in Wake County, sensors A6302 and A6301 in Nash County, sensor A4201 in Harnett County, sensors A5001D4 and R5001 in Johnston County, and sensor R3103 in Durham County form one significant cluster, and all those sensors are located in the same county or adjacent counties. Similarly, sensors A9501,

A3003, A7101, W7002, W2301, and A6401 form the second cluster, located in the neighboring counties in southeast North Carolina. The sensors in Hyde County and Dare County form the third cluster, and the fourth cluster consists of the only sensor (A9001) located in Vance County.

The topological association of the sensors is depicted in Figure 5.5 [40], where Wake County and its neighboring counties form the first cluster. The adjacent counties in southeastern North Carolina shown in brown color on the map are in the second cluster, and the easternmost counties (Dare and Hyde) form the third cluster. This implies that to predict the traffic volume at a location, we may need the historical traffic volumes at the same location and the traffic volumes at the locations in the same cluster.



Figure 5.5: Locations of sensor clusters on the North Carolina map

## FINDINGS, CONCLUSIONS, RECOMMENDATIONS

In this CATM project, we (1) identified road segments that are critical to the resiliency of road transportation system around Charlotte using weighted betweenness centrality and 2018 average daily traffic (AADT); (2) investigated the most affected airlines at the most affect airport during Hurricane Matthew and estimated the number of affected passengers during the hurricane using network theory; (3) proposed and tested a graph theoretical approach to analyzing the U.S. airport network during a hurricane disruption, and a rerouting method to identify feasible airports to reroute from a disrupted airport; (4) investigated significant cues for Evacuation Planners' decisions during hurricane evacuation using the Brunswik Linear Lens Model and the six machine learning algorithms; and (5) analyzed traffic flow data during Hurricane Florence evacuation in N.C. to discover space-time evacuation traffic patterns, and investigated the association of sensor locations to predict the hourly traffic during the hurricane evacuation.

For road transportation, our resiliency analysis showed that the central links with high AADT, such as road segments of U.S. Interstate 77 and U.S. Highway 74, are the most critical to the resiliency of the highway transportation network around Charlotte, and that road segments of U.S. Interstates 85 and 485 around Charlotte are also critical to the road network resiliency. For air transportation, our analysis of flight delays due to Hurricane Matthew revealed that seven airlines were most affected at the airport of MCO (which was the most affected airport), and that the topology of an airline's flight network may influence the number of flight passengers affected by a weather disruption. Based on this finding, a graph theoretical method, including two mathematical equations for disrupter and disruptee, respectively, has been proposed to quantify airports in an airport network from the two perspectives (disrupter and disruptee). Our testing results showed that there is a high chance for an airport to be geographically impacted by a hurricane disruption and the rerouting method can identify feasible airports for rerouting flights from the disruptees. The proposed graph theoretical and rerouting methods can support airports and airlines administrators to recognize the airports that might be affected by an approaching hurricane, and identify potential airports to divert flights from the affected airports.

For hurricane evacuation, the results of our evacuation traffic analysis showed that the sensor locations from the same county and adjacent counties form the cluster, and the traffic volume at a sensor location can be predicted by the traffic volumes in the same county and adjacent counties. Our results revealed that the 25 sensor locations could be grouped into four clusters. Wake County and its neighboring counties are grouped as the largest cluster, adjacent counties in southeast N.C. as the second-largest cluster, the easternmost counties (Dare and Hyde) as a cluster, and Vance County as the last cluster. Predicting the traffic volume at a location needs to consider historical traffic volumes at the same location and the locations in the same cluster. Our results of decision making cues for hurricane evacuation showed that among the seven cues we tested, only one cue (wind speed) contributes to Evacuation Planners' decision (i.e., whether to issue an evacuation order). The predictive models created in our studies can be used to manage hurricane evacuations, including proper traffic control, estimating emergency responders needed, and preparing enough evacuation supplies such as gas, water, food, and hotel rooms. These models and findings will help emergency response agencies deploy effective evacuation operations and improve the mobility of the people and evacuation resources during a hurricane.

## REFERENCES

1. Chemtob, D., Off, G. (2019). Charlotte jumps in rankings of largest U.S. cities, surpassing Indianapolis. Retrieved from The Charlotte Observer. Website: <https://www.charlotteobserver.com/news/business/biz-columns-blogs/development/article230790609.html>
2. Schrank, D., Eisele, B., Lomax, T. (2019). 2019 Urban Mobility Report. Retrieved from Texas A&M Transportation Institute Website: <https://static.tti.tamu.edu/tti.tamu.edu/documents/mobility-report-2019.pdf>
3. Brandes, U. (2001). A faster algorithm for betweenness centrality. *The Journal of Mathematical Sociology*, 25(2), 312-340.
4. Girvan M, Newman ME (2002) Community structure in social and biological networks. *Proc Natl Acad Sci USA* 99(12):7821–7826.
5. Annual Passengers on All U.S. Scheduled Airline Flights (Domestic & International) and Foreign Airline Flights to and from the United States, 2003-2017. (2019, September 25). Retrieved October 1, 2019, from <https://www.bts.gov/>.
6. 2016-economic-impact-report FINAL.pdf. (2019, July 25). Retrieved October 1, 2019, from <https://www.faa.gov/>.
7. Kohl, N., Larsen, A., Larsen, J., Ross, A., & Tiourine, S. (2007). Airline disruption management—perspectives, experiences and outlook. *Journal of Air Transport Management*, 13(3), 149-162.
8. Wei, G., Yu, G., & Song, M. (1997). Optimization model and algorithm for crew management during airline irregular operations. *Journal of Combinatorial Optimization*, 1(3), 305-321.
9. Bratu, S., & Barnhart, C. (2006). Flight operations recovery: New approaches considering passenger recovery. *Journal of Scheduling*, 9(3), 279-298.
10. Petersen, J. D., Sölveling, G., Clarke, J. P., Johnson, E. L., & Shebalov, S. (2012). An optimization approach to airline integrated recovery *Transportation Science*, 46(4), 482-500.
11. OAG Aviation Worldwide Limited, OAG. 2018.
12. Center, N. H. (2001, January 1). National Hurricane Center Tropical Cyclone Report Hurricane Matthew (AL142016). Retrieved October 1, 2019, from <https://www.nhc.noaa.gov/>.
13. Hurricane Matthew – Virginia Impacts. (n.d.). Retrieved October 1, 2019, from <http://dls.virginia.gov/>.
14. Hagberg, A., Swart, P., & Chult, D.S. (2008). Exploring network structure, dynamics, and function using NetworkX. Los Alamos National Lab. (LANL), Los Alamos, NM (United States).

15. Load Factor (passenger-miles as a proportion of available seat-miles in percent) All Carriers - All Airports. (2019, September 25). Retrieved October 1, 2019, from <https://www.bts.gov/>.
16. Harshitha Meda, Lauren B Davis, and Chrysafis Vogiatzis. “Analysis of Hurricane Matthew 2016 Data to Estimate Airline Passengers Disruption”. In: 2019 IEEE International Conference on Big Data (Big Data). IEEE. 2019, pp. 3909–3915.
17. Cook, G. N., & Goodwin, J. (2008). Airline Networks: A comparison of hub-and-spoke and point-to-point systems. *Journal of Aviation Aerospace Education & Research*, 17(2), 1.
18. Bounova, G. A. (2009). Topological evolution of networks: case studies in the US airlines and language Wikipedias (Doctoral dissertation, Massachusetts Institute of Technology).
19. Amy Cohn. How the Passenger Aviation Industry Prepares for and Responds to Disruptions: Foundational Analysis and Current-State Assessment Part. 2016.
20. BTS. Understanding the Reporting of Causes of Flight Delays and Cancellations @ONLINE. Mar. 2020. url: <https://www.bts.gov/topics/airlines-andairports/understanding-reporting-causes-flight-delays-and-cancellations>.
21. Martinhugo. Airlines cancel nearly 5,000 flights because of Hurricane Irene @ONLINE. Aug. 2011. url: <https://www.latimes.com/travel/la-xpm-2011-aug-27-la-me-0827-flights-cancel-20110828-story.html>.
22. Nicasjack. Hurricane Sandy Forces More Than 12,000 Flight Cancellations @ONLINE. Oct. 2012. url: <https://www.wsj.com/articles/SB10001424052970204840504578086833916411390>.
23. Sepehr Sarmadi. “Minimizing airline passenger delay through integrated flight scheduling and aircraft routing”. PhD thesis. Massachusetts Institute of Technology, 2004.
24. FAA. Sept. 2019. url: <https://www.faa.gov/news/updates/?newsId=94486>.
25. Curtis Tate. Airlines react to Iran tensions by rerouting flights; FAA orders US carriers to avoid airspace. Jan. 2020. url: <https://www.usatoday.com/story/travel/news/2020/01/10/iran-plane-crash-airlines-reroute-flights-faa-avoid-airspace/4429347002/>.
26. Christian M Schneider et al. “Mitigation of malicious attacks on networks”. In: *Proceedings of the National Academy of Sciences* 108.10 (2011), pp. 3838–3841.
27. Xiaoqian Sun, Volker Gollnick, and Sebastian Wandelt. “Robustness analysis metrics for worldwide airport network: A comprehensive study”. In: *Chinese Journal of Aeronautics* 30.2 (2017), pp. 500–512.
28. Massimiliano Zanin and Fabrizio Lillo. “Modelling the air transport with complex networks: A short review”. In: *The European Physical Journal Special Topics* 215.1 (2013), pp. 5–21.

29. Meda, H. (2021). A Theoretical Approach and Optimization Model integrating Network Theory to Analyze and Mitigate Airport Network Disruption. Dissertation, North Carolina A&T State University, Greensboro, North Carolina.
30. Guido Van Rossum and Fred L Drake Jr. Python reference manual. Centrum voor Wiskunde en Informatica Amsterdam, 1995.
31. Simonovic, S. P., & Ahmad, S. (2005). Computer-based model for flood evacuation emergency planning. *Natural Hazards*, 34(1), 25-51.
32. Whitehead, J. C., Edwards, B., Van Willigen, M., Maiolo, J. R., Wilson, K., & Smith, K. T. (2000). Heading for higher ground: factors affecting real and hypothetical hurricane evacuation behavior. *Global Environmental Change Part B: Environmental Hazards*, 2(4), 133-142.
33. Hasan, S., Ukkusuri, S., Gladwin, H., & Murray-Tuite, P. (2011). Behavioral model to understand household-level hurricane evacuation decision making. *Journal of Transportation Engineering*, 137(5), 341-348.
34. Fu, H., & Wilmot, C. G. (2006). Survival analysis-based dynamic travel demand models for hurricane evacuation. *Transportation Research Record*, 1964(1), 211-218.
35. North Carolina Department of Safety, WebEOC database 2016, [www.ncsparta.net/eoc7/default.aspx](http://www.ncsparta.net/eoc7/default.aspx). Accessed July 15, 2019.
36. Cooksey, R. W. (1996). *Judgment analysis: Theory, methods, and applications*. Academic Press.
37. The Centre for Research on the Epidemiology of Disasters, Annual Disaster Statistical Review 2019, [www.emdat.be/sites/default/files/adsr\\_2019.pdf](http://www.emdat.be/sites/default/files/adsr_2019.pdf). Accessed Nov-30, 2020.
38. North Carolina Department of Transportation website link for divisions <https://connect.ncdot.gov/resources/State-Mapping/Pages/Division-Map.aspx>, 2020. Accessed Nov-30, 2020.
39. Hastie, T., Tibshirani, R., James, G., & Witten, D. (2013). An introduction to statistical learning with applications in R.
40. An open source website to draw the map, website:[diymaps.net/nc](http://diymaps.net/nc). Accessed, Nov-30 2020.

## APPENDIX A: Data for Hurricane Evacuation in North Carolina

Table A.1: Data obtained from multiple sources for the judgment model

Name of County	No of Shelters	Wind Speed	Rainfall	Households affected	Flood Level (ft)	Median Household Income	Poverty Percent	Evacuate
Anson	1	45	4	74	24.39	33,228	25.1	0
Beaufort	2	50	7.5	850	12.50	45,860	19	1
Bertie	2	40	10.5	1025	16.67	34,127	24.4	0
Bladen	4	39	12	2817	36.34	34,422	26.4	0
Brunswick	3	67	7	784	18.98	47,000	13.8	0
Carteret	2	60	6.5	49	8.48	52,000	12.3	1
Columbus	5	59	11.5	5189	2.00	40,000	24.6	0
Cumberland	6	60	13	14803	58.70	42,107	18.8	0
Dare	0	75	6	1121	3.00	56,489	10.9	1
Duplin	3	49	7	1322	19.92	39,146	21.3	0
Durham	1	60	11.5	850	17.73	54,093	16.1	0
Edgecombe	4	60	11.5	3139	36.15	35,000	23.9	1
Franklin	0	45	8.41	13	23.18	50,000	15.3	0
Gates	0	64	9	158	16.19	49,258	15.2	0
Greene	1	50	9	579	24.18	38,010	23.7	0
Harnett	1	57	7	1683	19.31	51,682	16.1	0
Hyde	0	75	6	194	2.00	56,285	22.3	1
Hertford	1	40	9	453	15.40	37,000	26.1	0
Hoke	1	60	11.5	1786	12.84	45,829	19.5	0
Johnston	3	50	11.5	1683	28.90	57,151	13.2	0
Jones	1	50	6.5	226	18.46	34,005	21.5	0
Lee	1	45	11.5	190	11.44	50,547	16.9	0
Lenoir	1	51	9	3291	28.24	38,000	20.6	1
Martin	1	50	9	213	11.60	35,080	22.5	0
Montgomery	0	50	4	0	10.40	37,800	21.4	0
Moore	1	55	5	343	8.91	56,678	11.4	0
Nash	1	55	7	927	15.26	47,200	16.5	0
New Hanover	1	75	6	23	3.00	56,200	17.3	0
Onslow	6	50	6.5	442	20.55	38,000	13.7	0
Orange	1	45	6.5	850	16.25	61,130	12.8	0
Pamlico	1	50	5	7569	2.00	46,762	18.5	0
Pasquotank	1	64	8.5	476	16.19	45,400	17	0
Pender	3	68	6	957	17.79	50,000	15	1
Pitt	3	69	8	3303	24.46	50,000	21.5	1
Richmond	0	50	6	23	17.60	37,000	24.9	0
Robeson	5	67	11	18482	25.00	33,000	27.8	1



Table A.1: (cont'd)

<b>Name of County</b>	<b>No of Shelters</b>	<b>Wind Speed</b>	<b>Rainfall</b>	<b>Households affected</b>	<b>Flood Level (ft)</b>	<b>Median Household Income</b>	<b>Poverty Percent</b>	<b>Evacuate</b>
Sampson	3	60	12	2236	27.92	38,835	19.6	0
Scotland	0	55	7	500	15.47	52,000	27.6	0
Vance	1	55	5	850	2.00	32,733	24.2	0
Wake	1	45	9	916	5.47	76,000	9.2	0
Wayne	3	50	6.5	6695	2.00	45,000	20.6	1
Wilson	1	52.5	10.5	721	2.00	43,456	22.3	0

Table A.2: Summary of evacuation traffic data in eastern North Carolina

Sr.No	File name	District	County	Location	Location ID	Route
1	A2702	1	Dare	US 64 Hwy	280000002	64
2	A3002	3	Duplin	W NC 24 Hwy	0310000003	24
3	A3003	3	Duplin	E NC 24 Hwy	0310000002	24
4	A5001	4	Johnston	I-40	0510000001	40
5	A5301	2	Lenoir	Hwy 55 W	0540000001	55
6	A6401	3	New Hanover	Castle Hayne Rd	0650000001	117
7	A6403	3	New Hanover	Wrightsville Ave	0650000002	74
8	A7101	3	Pender	US Hwy 421	0710000002	421
9	R0901	3	Brunswick	Ocean Hwy W	0100000428	17
10	R1401	1	Camden	US 17	0150000003	17
11	R2301	6	Columbus	N US 701 Bypass	0240000676	701
12	R2701	1	Dare	NC 12 Hwy	280000004	12
13	R5001	4	Johnston	I-95	0510000002	95
14	R5301	2	Lenoir	Hwy 70 W	0540000002	70
15	W2301	6	Columbus	Andrew Jackson Hwy E	0240000001	74
16	W4701	1	Hyde	US 264 Hwy	0480000001	264
17	W7002	3	Pender	US hwy 421	0710000002	421
18	A2501	6	Cumberland	All American Exp	0260000001	1007
19	A4201	6	Harnett	E Cornelius Harnett Blvd	0430000001	421
20	A5001	4	Johnston	I-40	0510000001	40
21	A6301	4	Nash	US 264 E	0640000005	264
22	A6302	4	Nash	W NC 97	0640000003	97
23	A9001	5	Vance	S Carroll St	0910000001	1501
24	A9501	4	Wayne	US 117 Alternate	0960000001	117
25	R3103	5	Durham	I-40 E	0320000010	40
26	R3201	4	Edgecombe	US 64 East	0330000002	64
27	R6301	4	Nash	US 64 East	0640000006	64
28	R7701	6	Robeson	I-74 E	0780000002	74
29	R9101	5	Wake	US 70 Hwy E	0920000081	70
30	R9102	5	Wake	Capital Blvd	0920000082	401
31	R9103	5	Wake	I-40 EB	0920000013	40
32	R9104	5	Wake	I-40 EB	0920000014	40
33	R9106	5	Wake		0920000020	440
34	R9107	5	Wake	I 540 EB	920000024	540
35	R9108	5	Wake	I 440 EB	0920000021	440
36	R9111	5	Wake	I 40 EB	0920000016_EB	40
37	R9112	5	Wake	I 40 EB	0920000017	40
38	R9113	5	Wake	I 40 EB	0920000018	40
39	R9114	5	Wake	I 540 EB	0920000025	540

## APPENDIX B: Codes for Prediction Models of Hurricane Evacuation Traffic in Eastern North Carolina

```

## Libraries required for analysis
# importing libraries
import pandas as pd
import matplotlib.pyplot as plt
import statsmodels.api as sm
from scipy.stats import normaltest
from scipy.stats import shapiro
from scipy.stats import anderson

# # Data for the analysis
def DailyTraffic(TData, Date):
    df1 = TData[TData['DATE'] == Date]

    df2 = df1.drop(['DIST','DIR', 'DATE'], axis=1)
    df3 = df2.sort_index()
    df4 = df3[~df3.index.duplicated()]
    df5 = df4.T

    Hours = pd.Series(list(range(1,25)),index=df5.index)
    df5['Hour'] = Hours
    return df5
# End of DailyTraffic

# Function to add shifted traffic data to the dataset
def addShiftTraffic(DataSet, OneSiteTraffic, periods = 4):
    for i in range(1, periods+1):
        ShiftedTraffic = OneSiteTraffic.shift(periods=i)
        ColumnSuffix = '_' +str(i) + 'HrBf'
        DataSet = DataSet.join(ShiftedTraffic, rsuffix=ColumnSuffix)

    return DataSet

Folder = "C:/Users/shmhatre/Desktop/Spring_2020/CATM
project_2020/TrafficEvacAnalysis/Sensor_Analysis/"

Counties = pd.read_csv(Folder + "AdjacentCounty.csv", index_col="County")
Counties['Sr.No'] = Counties.index

SensorSite = pd.read_csv(Folder + "Consolidate Data.csv", index_col="SITE")

D1 = pd.read_csv(Folder + "D1.csv",index_col='SITE')
D2 = pd.read_csv(Folder + "D2.csv",index_col='SITE')
D3 = pd.read_csv(Folder + "D3.csv",index_col='SITE')
D4 = pd.read_csv(Folder + "D4.csv",index_col='SITE')
D5 = pd.read_csv(Folder + "D5.csv",index_col='SITE')
D6 = pd.read_csv(Folder + "D6.csv",index_col='SITE')

```

```

# Merge the traffic data from all files
# Then separate them into four datasets by directions
RawData = pd.concat([D1,D2,D3,D4,D5,D6], sort=False)
EBTraffic = RawData[RawData['DIR'] == 'EB']
WBTraffic = RawData[RawData['DIR'] == 'WB']
NBTraffic = RawData[RawData['DIR'] == 'NB']
SBTraffic = RawData[RawData['DIR'] == 'SB']

# Filter the evacuation data and re-organize the dataset
Dates = ['9/5/2018', '9/6/2018', '9/7/2018', '9/8/2018', '9/9/2018']

WBframes = [0] * len(Dates)
NBframes = [0] * len(Dates)

for i in range(len(Dates)):
    WBframes[i] = DailyTraffic(WBTraffic, Dates[i])
    NBframes[i] = DailyTraffic(NBTraffic, Dates[i])

WBTDData = pd.concat(WBframes, keys=Dates, sort=False)
NBTDData = pd.concat(NBframes, keys=Dates, sort=False)

EvacuationTraffic = WBTDData.join(NBTDData, how='outer', rsuffix='_NB')

# Prepare the dataset for the prediction modeling
# PredInput is the dataset for the prediction modeling
AvailableSensors = list(EvacuationTraffic.columns)
Sensor = "R9103"

PredInput = EvacuationTraffic.loc[:, [Sensor, 'Hour']]

SiteTraffic = EvacuationTraffic[Sensor]
PredInput = addShiftTraffic(PredInput, SiteTraffic)

SensorCounty = SensorSite.loc[Sensor, 'County']

for adjCounty in Counties.loc[SensorCounty]:
    adjSensors = SensorSite[SensorSite['County'] == adjCounty].index

    for adjSensor in adjSensors:
        if adjSensor == Sensor:
            continue

        print(adjSensor)
        available = AvailableSensors.count(adjSensor)
        if available == 0:
            print('Sensor ' + adjSensor + ' is missing!')
        elif available == 1:
            adjTraffic = EvacuationTraffic[adjSensor]

```

```

PredInput = PredInput.join(adjTraffic)
PredInput = addShiftTraffic(PredInput, adjTraffic)
PredInput = PredInput.drop([adjSensor], axis=1)

Df1 = PredInput.iloc[3:,]
Df1
Data = Df1.dropna(axis=1)
X = Data.drop(['R9103','Hour'] ,axis=1)
y = Data['R9103']

# Adding constant column of ones, mandatory for sm.OLS model
X_1 = sm.add_constant(X)

# Fitting sm.OLS model
model = sm.OLS(y,X_1).fit()

# Backward Elimination
cols = list(X.columns)
pmax = 1
while (len(cols)>0):
    p= []
    X_1 = X[cols]
    X_1 = sm.add_constant(X_1)
    model = sm.OLS(y,X_1).fit()
    p = pd.Series(model.pvalues.values[1:],index = cols)
    pmax = max(p)
    feature_with_p_max = p.idxmax()
    if(pmax>0.05):
        cols.remove(feature_with_p_max)
    else:
        break
selected_features_BE = cols
print(selected_features_BE)

# Adding constant column of ones, mandatory for sm.OLS model
X_1 = sm.add_constant(X)

# Fitting sm.OLS model
model = sm.OLS(y,X_1).fit()

# model.pvalues

X2 = sm.add_constant(X)
model = sm.OLS(y, X2)
result = model.fit()
res = result.resid
fig = sm.qqplot(res,fit=True,line ='45')
h = plt.title('Normal QQ Plot ' +Sensor)

```

```
plt.savefig("C:/Users/shmhatre/Desktop/Spring_2020/CATM
project_2020/TrafficEvacAnalysis/Informs_result/" + Sensor+'_qqplot.png',transparent =
True, dpi= 1000, bbox_inches ='tight')
plt.show()

# output residual
res
res.to_excel("C:/Users/shmhatre/Desktop/Spring_2020/CATM
project_2020/TrafficEvacAnalysis/Sensor_Analysis/" + "res" + Sensor + ".xlsx")

# Shapiro-Wilk Test
data = res

# normality test
stat, p = shapiro(data)
print('Statistics=%.3f, p=%.3f % (stat, p))

# interpret
alpha = 0.05
if p > alpha:
    print('Sample looks Gaussian (fail to reject H0)')
else:
    print('Sample does not look Gaussian (reject H0)')

# D'Agostino and Pearson's Test
data = res

# normality test
stat, p = normaltest(data)
print('Statistics=%.3f, p=%.3f % (stat, p))

# interpret
alpha = 0.05
if p > alpha:
    print('Sample looks Gaussian (fail to reject H0)')
else:
    print('Sample does not look Gaussian (reject H0)')

# generate univariate observations
data = res

# normality test
result = anderson(data)
print('Statistic: %.3f % result.statistic)
p = 0
for i in range(len(result.critical_values)):
    sl, cv = result.significance_level[i], result.critical_values[i]
    if result.statistic < result.critical_values[i]:
```

```

        print('%0.3f: %0.3f, data looks normal (fail to reject H0)' % (sl, cv))
    else:
        print('%0.3f: %0.3f, data does not look normal (reject H0)' % (sl, cv))

# Visualisation for Cook's distance (CD) to identify the most influential observation in outlier detection

# Instantiate and fit the visualizer
# with ('9/5/2018', 'HR 9'),('9/6/2018', 'HR 8'),('9/8/2018', 'HR 19'),('9/8/2018', 'HR 22') dropping
from yellowbrick.regressor import CooksDistance
visualizer = CooksDistance()
visualizer.fit(X, y)
visualizer.show()

# Adding constant column of ones, mandatory for sm.OLS model
X_1 = sm.add_constant(X)
# Fitting sm.OLS model
model = sm.OLS(y,X_1).fit()

infl = model.get_influence()
sm_fr = infl.summary_frame()
sm_fr

sm_fr.to_excel("C:/Users/shmhatre/Desktop/Spring_2020/CATM
project_2020/TrafficEvacAnalysis/Sensor_Analysis/" + "CD" + Sensor + ".xlsx")

X.drop([('9/5/2018', 'HR 6'), ('9/5/2018', 'HR 7'),('9/6/2018', 'HR 6'),('9/6/2018', 'HR 7'),
('9/6/2018', 'HR 17'),
('9/7/2018', 'HR 6'),('9/7/2018', 'HR 7'),('9/8/2018', 'HR 19'),('9/8/2018', 'HR 20')],axis=0,
inplace=True)

y.drop([('9/5/2018', 'HR 6'), ('9/5/2018', 'HR 7'),('9/6/2018', 'HR 6'),('9/6/2018', 'HR 7'),
('9/6/2018', 'HR 17'),
('9/7/2018', 'HR 6'),('9/7/2018', 'HR 7'),('9/8/2018', 'HR 19'),('9/8/2018', 'HR 20')],axis=0,
inplace=True)

from yellowbrick.regressor import CooksDistance
visualizer = CooksDistance()
visualizer.fit(X, y)
visualizer.show()

#Adding constant column of ones, mandatory for sm.OLS model
X_1 = sm.add_constant(X)
#Fitting sm.OLS model
model = sm.OLS(y,X_1).fit()
#model.pvalues

sm_fr.to_excel("C:/Users/shmhatre/Desktop/Spring_2020/CATM
project_2020/TrafficEvacAnalysis/Sensor_Analysis/" + "7RS" + Sensor + ".xlsx")

```

```
X2 = sm.add_constant(X)
model = sm.OLS(y, X2)
result = model.fit()
res = result.resid
fig = sm.qqplot(res, fit=True, line='45')
#probplot = sm.ProbPlot(res)
# fig = probplot.qqplot()
h = plt.title('Normal QQ Plot 9RES ' + Sensor)
plt.savefig("C:/Users/shmhatre/Desktop/Spring_2020/CATM
            project_2020/TrafficEvacAnalysis/Informs_result/" +
            Sensor+'_qqplot.png', transparent = True, dpi= 1000, bbox_inches='tight')
plt.show()

# Shapiro-Wilk Test

data = res
# normality test
stat, p = shapiro(data)
print('Statistics=%.3f, p=%.3f % (stat, p))
# interpret
alpha = 0.05
if p > alpha:
    print('Sample looks Gaussian (fail to reject H0)')
else:
    print('Sample does not look Gaussian (reject H0)')

# D'Agostino and Pearson's Test
from scipy.stats import normaltest
data = res
# normality test
stat, p = normaltest(data)
print('Statistics=%.3f, p=%.3f % (stat, p))
# interpret
alpha = 0.05
if p > alpha:
    print('Sample looks Gaussian (fail to reject H0)')
else:
    print('Sample does not look Gaussian (reject H0)')

# generate univariate observations
data = res
# normality test
result = anderson(data)
print('Statistic: %.3f % result.statistic)
p = 0
for i in range(len(result.critical_values)):
```

```
sl, cv = result.significance_level[i], result.critical_values[i]
if result.statistic < result.critical_values[i]:
    print('%0.3f: %0.3f, data looks normal (fail to reject H0)' % (sl, cv))
else:
    print('%0.3f: %0.3f, data does not look normal (reject H0)' % (sl, cv))

# After passing the normality check we accept the data and do the analysis for other sensors
```

## APPENDIX C: Posters and Presentation Slides

### Judgment Model Characterization for Emergency Evacuation Using Lens Model: A Machine Learning Approach

Miriam Alabi<sup>1</sup>, Younho Seong<sup>1</sup>, Sun Y<sup>2</sup>

<sup>1</sup>Department of Industrial and System Engineering, <sup>2</sup>Department of Mechanical Engineering  
<sup>1</sup>North Carolina A&T State University, Greensboro, North Carolina

#### Introduction

Intelligent Transportation Systems play an important role in many emergency situations. In this context, one purpose to characterize the decision making behavior during evacuation using machine learning algorithms. Also, a decision-making tool, Brunswick Lens model is used to describe the correlation between the prediction and the behavior of organisms in the environment. Prediction is made when an individual or individuals make critical decisions based on multiple cues using Brunswick data in a case study. In the modeling process, a judgment model and an ecological model will be created. Identify significant cues for residents in deciding dynamic evacuation routes when the environment changes and incomplete information. The goal is to create a judgment model for emergency to gain insight into the decision behavior of the various entities involved when the environment presents multiple cues.

Whithead et al. (2001), Fu and Whitson (2004), Fu et al. (2006), Hsuan et al. (2011) considered the variables wind speed, rainfall, number of households affected, flood level, median household income and the poverty level. These variables (cues) were found to influence evacuation in North Carolina while preparing for an impending hurricane were adapted.

#### Decision Making Tool – Lens Model

Brunswick Lens model is used to describe the relationship between the environment and the behavior of organisms in the environment.

$$A_i = Cor(C_i, P_i)$$

$$C = Cor(C_1, C_2, \dots, C_n)$$

$$P = Cor(P_1, P_2, \dots, P_n)$$

$$L = Cor(C, P) = \sqrt{1 - R^2}$$

#### Machine learning

Machine Learning algorithms:

- Python packages provides algorithms built in their libraries.
- Supervised learning is a machine learning technique where algorithms were used to learn the mapping function from the input to the output.
- Six (6) machine learning algorithms were also used to create the judgment model namely linear discriminant analysis (LDA), K-nearest neighbor (KNN), Logistic regression (LR), Classification and regression tree (Decision tree)(CART), Naïve-Bayes (NB), support vector machine (SVM).

#### Conclusion

- Logistic regression using the Lens model provided a better estimation of judgment modelling with a model accuracy of 0.84.
- The supervised machine learning techniques, LR, LDA, KNN, CART, NB, SVM also showed interesting accuracies but did not perfectly estimate the judgment model since model accuracies were 0.66, 0.69, 0.69, 0.69, 0.65 and 0.758 respectively.

#### Future Work

The ecological model from the environment is not available hence there is no data to help create the model. In this study Monte-Carlo simulation (MCS) will be used to generate data to create the ecological model in order to fully build the lens model for this emergency situation.

#### Acknowledgement

The authors would like to thank Center for Advanced Transportation Mobility, for financially supporting this research under grant No. 69A3551747125. We are also grateful to the North Carolina A&T State University for providing the infrastructure.

#### Methods

There was no high positive correlations between the cues indicating that all cues are independent and can be used for predictions

Figure 2 shows Correlation matrix between the cues

#### Results

Figure 3 shows the sequence of estimating the significant cues

#### Machine learning algorithms

Accuracy (lens model) =  $\frac{TP+TN}{TP+TN+FP+FN} = \frac{113}{135} = 0.84$

Figure 4 shows the confusion matrix

	Actual True Positive (0.4)	Actual False Negative (0.6)
Predicted (P)	True Positive (0.03)	True Negative (0.97)

Figure 5 shows the algorithms and their accuracies



# Characterization of Emergency evacuation with the lens model Using Machine Learning and Monte Carlo Simulation

Cross-Disciplinary Research Area:  
Human factors, Neuro-Science, Decision  
making, Simulation

Student(s): Miriam Alabi (PhD), Advisor(s): Dr. Younho Seong

## Introduction

Preparing for emergencies reduces significant losses to infrastructure and the economy. In emergency evacuation planning and operations, inputs from various decision-makers are involved, such as individuals/households and the government (evacuation managers and transport planners). The Lens Model (LM) has been used in analyses of judgment strategies to acknowledge the inherent probabilistic relationships between the criterion and the subject judgments (Brehmer, 1990 and Hammond et al., 1997).

Wind speed, rainfall, number of households affected, flood level, median household income and the poverty level on evacuation during emergencies were variables considered to affect evacuation during emergencies (Whithead et al., 2000; Fu & Wilmore 2004; Fu & Wilmore 2006; Husein et al., 2011).

In this situation, the criterion is unknown and uncertain, leaving the LM to replicate a single system design (design with incomplete information). This creates limitations within the LM framework in terms of understanding and determining how well judgments correspond to the ecology of criterion.

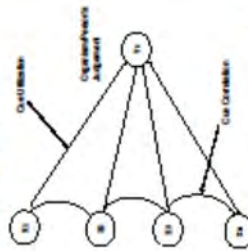


Figure 1 shows the framework: Lens Model (Single-System Design)

## Objective

This study, seeks to analyze the decision-making behavior during an emergency evacuation in an incomplete information environment. First, Monte-Carlo Simulation (MCS) is used to simulate the unwell-being/ecology/criterion data to facilitate the complete development of the judgment model. Secondly, the non-linear SML algorithms and the LM parameters are evaluated and compared to validate their performance.

## Methods

### Decision Making Tool – Lens Model

from Brehmer (1990)

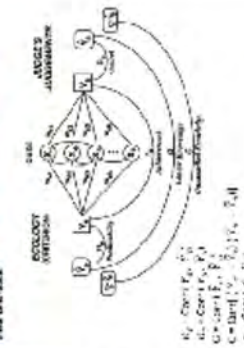


Figure 2 shows the framework: Lens Model (Double System Design)

The LM parameters are given by:  $\beta_0, \beta_1, \beta_2, \beta_3, \beta_4, \beta_5, \beta_6, \beta_7, \beta_8, \beta_9, \beta_{10}, \beta_{11}, \beta_{12}, \beta_{13}, \beta_{14}, \beta_{15}, \beta_{16}, \beta_{17}, \beta_{18}, \beta_{19}, \beta_{20}, \beta_{21}, \beta_{22}, \beta_{23}, \beta_{24}, \beta_{25}, \beta_{26}, \beta_{27}, \beta_{28}, \beta_{29}, \beta_{30}, \beta_{31}, \beta_{32}, \beta_{33}, \beta_{34}, \beta_{35}, \beta_{36}, \beta_{37}, \beta_{38}, \beta_{39}, \beta_{40}, \beta_{41}, \beta_{42}, \beta_{43}, \beta_{44}, \beta_{45}, \beta_{46}, \beta_{47}, \beta_{48}, \beta_{49}, \beta_{50}, \beta_{51}, \beta_{52}, \beta_{53}, \beta_{54}, \beta_{55}, \beta_{56}, \beta_{57}, \beta_{58}, \beta_{59}, \beta_{60}, \beta_{61}, \beta_{62}, \beta_{63}, \beta_{64}, \beta_{65}, \beta_{66}, \beta_{67}, \beta_{68}, \beta_{69}, \beta_{70}, \beta_{71}, \beta_{72}, \beta_{73}, \beta_{74}, \beta_{75}, \beta_{76}, \beta_{77}, \beta_{78}, \beta_{79}, \beta_{80}, \beta_{81}, \beta_{82}, \beta_{83}, \beta_{84}, \beta_{85}, \beta_{86}, \beta_{87}, \beta_{88}, \beta_{89}, \beta_{90}, \beta_{91}, \beta_{92}, \beta_{93}, \beta_{94}, \beta_{95}, \beta_{96}, \beta_{97}, \beta_{98}, \beta_{99}, \beta_{100}, \beta_{101}, \beta_{102}, \beta_{103}, \beta_{104}, \beta_{105}, \beta_{106}, \beta_{107}, \beta_{108}, \beta_{109}, \beta_{110}, \beta_{111}, \beta_{112}, \beta_{113}, \beta_{114}, \beta_{115}, \beta_{116}, \beta_{117}, \beta_{118}, \beta_{119}, \beta_{120}, \beta_{121}, \beta_{122}, \beta_{123}, \beta_{124}, \beta_{125}, \beta_{126}, \beta_{127}, \beta_{128}, \beta_{129}, \beta_{130}, \beta_{131}, \beta_{132}, \beta_{133}, \beta_{134}, \beta_{135}, \beta_{136}, \beta_{137}, \beta_{138}, \beta_{139}, \beta_{140}, \beta_{141}, \beta_{142}, \beta_{143}, \beta_{144}, \beta_{145}, \beta_{146}, \beta_{147}, \beta_{148}, \beta_{149}, \beta_{150}, \beta_{151}, \beta_{152}, \beta_{153}, \beta_{154}, \beta_{155}, \beta_{156}, \beta_{157}, \beta_{158}, \beta_{159}, \beta_{160}, \beta_{161}, \beta_{162}, \beta_{163}, \beta_{164}, \beta_{165}, \beta_{166}, \beta_{167}, \beta_{168}, \beta_{169}, \beta_{170}, \beta_{171}, \beta_{172}, \beta_{173}, \beta_{174}, \beta_{175}, \beta_{176}, \beta_{177}, \beta_{178}, \beta_{179}, \beta_{180}, \beta_{181}, \beta_{182}, \beta_{183}, \beta_{184}, \beta_{185}, \beta_{186}, \beta_{187}, \beta_{188}, \beta_{189}, \beta_{190}, \beta_{191}, \beta_{192}, \beta_{193}, \beta_{194}, \beta_{195}, \beta_{196}, \beta_{197}, \beta_{198}, \beta_{199}, \beta_{200}, \beta_{201}, \beta_{202}, \beta_{203}, \beta_{204}, \beta_{205}, \beta_{206}, \beta_{207}, \beta_{208}, \beta_{209}, \beta_{210}, \beta_{211}, \beta_{212}, \beta_{213}, \beta_{214}, \beta_{215}, \beta_{216}, \beta_{217}, \beta_{218}, \beta_{219}, \beta_{220}, \beta_{221}, \beta_{222}, \beta_{223}, \beta_{224}, \beta_{225}, \beta_{226}, \beta_{227}, \beta_{228}, \beta_{229}, \beta_{230}, \beta_{231}, \beta_{232}, \beta_{233}, \beta_{234}, \beta_{235}, \beta_{236}, \beta_{237}, \beta_{238}, \beta_{239}, \beta_{240}, \beta_{241}, \beta_{242}, \beta_{243}, \beta_{244}, \beta_{245}, \beta_{246}, \beta_{247}, \beta_{248}, \beta_{249}, \beta_{250}, \beta_{251}, \beta_{252}, \beta_{253}, \beta_{254}, \beta_{255}, \beta_{256}, \beta_{257}, \beta_{258}, \beta_{259}, \beta_{260}, \beta_{261}, \beta_{262}, \beta_{263}, \beta_{264}, \beta_{265}, \beta_{266}, \beta_{267}, \beta_{268}, \beta_{269}, \beta_{270}, \beta_{271}, \beta_{272}, \beta_{273}, \beta_{274}, \beta_{275}, \beta_{276}, \beta_{277}, \beta_{278}, \beta_{279}, \beta_{280}, \beta_{281}, \beta_{282}, \beta_{283}, \beta_{284}, \beta_{285}, \beta_{286}, \beta_{287}, \beta_{288}, \beta_{289}, \beta_{290}, \beta_{291}, \beta_{292}, \beta_{293}, \beta_{294}, \beta_{295}, \beta_{296}, \beta_{297}, \beta_{298}, \beta_{299}, \beta_{300}, \beta_{301}, \beta_{302}, \beta_{303}, \beta_{304}, \beta_{305}, \beta_{306}, \beta_{307}, \beta_{308}, \beta_{309}, \beta_{310}, \beta_{311}, \beta_{312}, \beta_{313}, \beta_{314}, \beta_{315}, \beta_{316}, \beta_{317}, \beta_{318}, \beta_{319}, \beta_{320}, \beta_{321}, \beta_{322}, \beta_{323}, \beta_{324}, \beta_{325}, \beta_{326}, \beta_{327}, \beta_{328}, \beta_{329}, \beta_{330}, \beta_{331}, \beta_{332}, \beta_{333}, \beta_{334}, \beta_{335}, \beta_{336}, \beta_{337}, \beta_{338}, \beta_{339}, \beta_{340}, \beta_{341}, \beta_{342}, \beta_{343}, \beta_{344}, \beta_{345}, \beta_{346}, \beta_{347}, \beta_{348}, \beta_{349}, \beta_{350}, \beta_{351}, \beta_{352}, \beta_{353}, \beta_{354}, \beta_{355}, \beta_{356}, \beta_{357}, \beta_{358}, \beta_{359}, \beta_{360}, \beta_{361}, \beta_{362}, \beta_{363}, \beta_{364}, \beta_{365}, \beta_{366}, \beta_{367}, \beta_{368}, \beta_{369}, \beta_{370}, \beta_{371}, \beta_{372}, \beta_{373}, \beta_{374}, \beta_{375}, \beta_{376}, \beta_{377}, \beta_{378}, \beta_{379}, \beta_{380}, \beta_{381}, \beta_{382}, \beta_{383}, \beta_{384}, \beta_{385}, \beta_{386}, \beta_{387}, \beta_{388}, \beta_{389}, \beta_{390}, \beta_{391}, \beta_{392}, \beta_{393}, \beta_{394}, \beta_{395}, \beta_{396}, \beta_{397}, \beta_{398}, \beta_{399}, \beta_{400}, \beta_{401}, \beta_{402}, \beta_{403}, \beta_{404}, \beta_{405}, \beta_{406}, \beta_{407}, \beta_{408}, \beta_{409}, \beta_{410}, \beta_{411}, \beta_{412}, \beta_{413}, \beta_{414}, \beta_{415}, \beta_{416}, \beta_{417}, \beta_{418}, \beta_{419}, \beta_{420}, \beta_{421}, \beta_{422}, \beta_{423}, \beta_{424}, \beta_{425}, \beta_{426}, \beta_{427}, \beta_{428}, \beta_{429}, \beta_{430}, \beta_{431}, \beta_{432}, \beta_{433}, \beta_{434}, \beta_{435}, \beta_{436}, \beta_{437}, \beta_{438}, \beta_{439}, \beta_{440}, \beta_{441}, \beta_{442}, \beta_{443}, \beta_{444}, \beta_{445}, \beta_{446}, \beta_{447}, \beta_{448}, \beta_{449}, \beta_{450}, \beta_{451}, \beta_{452}, \beta_{453}, \beta_{454}, \beta_{455}, \beta_{456}, \beta_{457}, \beta_{458}, \beta_{459}, \beta_{460}, \beta_{461}, \beta_{462}, \beta_{463}, \beta_{464}, \beta_{465}, \beta_{466}, \beta_{467}, \beta_{468}, \beta_{469}, \beta_{470}, \beta_{471}, \beta_{472}, \beta_{473}, \beta_{474}, \beta_{475}, \beta_{476}, \beta_{477}, \beta_{478}, \beta_{479}, \beta_{480}, \beta_{481}, \beta_{482}, \beta_{483}, \beta_{484}, \beta_{485}, \beta_{486}, \beta_{487}, \beta_{488}, \beta_{489}, \beta_{490}, \beta_{491}, \beta_{492}, \beta_{493}, \beta_{494}, \beta_{495}, \beta_{496}, \beta_{497}, \beta_{498}, \beta_{499}, \beta_{500}, \beta_{501}, \beta_{502}, \beta_{503}, \beta_{504}, \beta_{505}, \beta_{506}, \beta_{507}, \beta_{508}, \beta_{509}, \beta_{510}, \beta_{511}, \beta_{512}, \beta_{513}, \beta_{514}, \beta_{515}, \beta_{516}, \beta_{517}, \beta_{518}, \beta_{519}, \beta_{520}, \beta_{521}, \beta_{522}, \beta_{523}, \beta_{524}, \beta_{525}, \beta_{526}, \beta_{527}, \beta_{528}, \beta_{529}, \beta_{530}, \beta_{531}, \beta_{532}, \beta_{533}, \beta_{534}, \beta_{535}, \beta_{536}, \beta_{537}, \beta_{538}, \beta_{539}, \beta_{540}, \beta_{541}, \beta_{542}, \beta_{543}, \beta_{544}, \beta_{545}, \beta_{546}, \beta_{547}, \beta_{548}, \beta_{549}, \beta_{550}, \beta_{551}, \beta_{552}, \beta_{553}, \beta_{554}, \beta_{555}, \beta_{556}, \beta_{557}, \beta_{558}, \beta_{559}, \beta_{560}, \beta_{561}, \beta_{562}, \beta_{563}, \beta_{564}, \beta_{565}, \beta_{566}, \beta_{567}, \beta_{568}, \beta_{569}, \beta_{570}, \beta_{571}, \beta_{572}, \beta_{573}, \beta_{574}, \beta_{575}, \beta_{576}, \beta_{577}, \beta_{578}, \beta_{579}, \beta_{580}, \beta_{581}, \beta_{582}, \beta_{583}, \beta_{584}, \beta_{585}, \beta_{586}, \beta_{587}, \beta_{588}, \beta_{589}, \beta_{590}, \beta_{591}, \beta_{592}, \beta_{593}, \beta_{594}, \beta_{595}, \beta_{596}, \beta_{597}, \beta_{598}, \beta_{599}, \beta_{600}, \beta_{601}, \beta_{602}, \beta_{603}, \beta_{604}, \beta_{605}, \beta_{606}, \beta_{607}, \beta_{608}, \beta_{609}, \beta_{610}, \beta_{611}, \beta_{612}, \beta_{613}, \beta_{614}, \beta_{615}, \beta_{616}, \beta_{617}, \beta_{618}, \beta_{619}, \beta_{620}, \beta_{621}, \beta_{622}, \beta_{623}, \beta_{624}, \beta_{625}, \beta_{626}, \beta_{627}, \beta_{628}, \beta_{629}, \beta_{630}, \beta_{631}, \beta_{632}, \beta_{633}, \beta_{634}, \beta_{635}, \beta_{636}, \beta_{637}, \beta_{638}, \beta_{639}, \beta_{640}, \beta_{641}, \beta_{642}, \beta_{643}, \beta_{644}, \beta_{645}, \beta_{646}, \beta_{647}, \beta_{648}, \beta_{649}, \beta_{650}, \beta_{651}, \beta_{652}, \beta_{653}, \beta_{654}, \beta_{655}, \beta_{656}, \beta_{657}, \beta_{658}, \beta_{659}, \beta_{660}, \beta_{661}, \beta_{662}, \beta_{663}, \beta_{664}, \beta_{665}, \beta_{666}, \beta_{667}, \beta_{668}, \beta_{669}, \beta_{670}, \beta_{671}, \beta_{672}, \beta_{673}, \beta_{674}, \beta_{675}, \beta_{676}, \beta_{677}, \beta_{678}, \beta_{679}, \beta_{680}, \beta_{681}, \beta_{682}, \beta_{683}, \beta_{684}, \beta_{685}, \beta_{686}, \beta_{687}, \beta_{688}, \beta_{689}, \beta_{690}, \beta_{691}, \beta_{692}, \beta_{693}, \beta_{694}, \beta_{695}, \beta_{696}, \beta_{697}, \beta_{698}, \beta_{699}, \beta_{700}, \beta_{701}, \beta_{702}, \beta_{703}, \beta_{704}, \beta_{705}, \beta_{706}, \beta_{707}, \beta_{708}, \beta_{709}, \beta_{710}, \beta_{711}, \beta_{712}, \beta_{713}, \beta_{714}, \beta_{715}, \beta_{716}, \beta_{717}, \beta_{718}, \beta_{719}, \beta_{720}, \beta_{721}, \beta_{722}, \beta_{723}, \beta_{724}, \beta_{725}, \beta_{726}, \beta_{727}, \beta_{728}, \beta_{729}, \beta_{730}, \beta_{731}, \beta_{732}, \beta_{733}, \beta_{734}, \beta_{735}, \beta_{736}, \beta_{737}, \beta_{738}, \beta_{739}, \beta_{740}, \beta_{741}, \beta_{742}, \beta_{743}, \beta_{744}, \beta_{745}, \beta_{746}, \beta_{747}, \beta_{748}, \beta_{749}, \beta_{750}, \beta_{751}, \beta_{752}, \beta_{753}, \beta_{754}, \beta_{755}, \beta_{756}, \beta_{757}, \beta_{758}, \beta_{759}, \beta_{760}, \beta_{761}, \beta_{762}, \beta_{763}, \beta_{764}, \beta_{765}, \beta_{766}, \beta_{767}, \beta_{768}, \beta_{769}, \beta_{770}, \beta_{771}, \beta_{772}, \beta_{773}, \beta_{774}, \beta_{775}, \beta_{776}, \beta_{777}, \beta_{778}, \beta_{779}, \beta_{780}, \beta_{781}, \beta_{782}, \beta_{783}, \beta_{784}, \beta_{785}, \beta_{786}, \beta_{787}, \beta_{788}, \beta_{789}, \beta_{790}, \beta_{791}, \beta_{792}, \beta_{793}, \beta_{794}, \beta_{795}, \beta_{796}, \beta_{797}, \beta_{798}, \beta_{799}, \beta_{800}, \beta_{801}, \beta_{802}, \beta_{803}, \beta_{804}, \beta_{805}, \beta_{806}, \beta_{807}, \beta_{808}, \beta_{809}, \beta_{810}, \beta_{811}, \beta_{812}, \beta_{813}, \beta_{814}, \beta_{815}, \beta_{816}, \beta_{817}, \beta_{818}, \beta_{819}, \beta_{820}, \beta_{821}, \beta_{822}, \beta_{823}, \beta_{824}, \beta_{825}, \beta_{826}, \beta_{827}, \beta_{828}, \beta_{829}, \beta_{830}, \beta_{831}, \beta_{832}, \beta_{833}, \beta_{834}, \beta_{835}, \beta_{836}, \beta_{837}, \beta_{838}, \beta_{839}, \beta_{840}, \beta_{841}, \beta_{842}, \beta_{843}, \beta_{844}, \beta_{845}, \beta_{846}, \beta_{847}, \beta_{848}, \beta_{849}, \beta_{850}, \beta_{851}, \beta_{852}, \beta_{853}, \beta_{854}, \beta_{855}, \beta_{856}, \beta_{857}, \beta_{858}, \beta_{859}, \beta_{860}, \beta_{861}, \beta_{862}, \beta_{863}, \beta_{864}, \beta_{865}, \beta_{866}, \beta_{867}, \beta_{868}, \beta_{869}, \beta_{870}, \beta_{871}, \beta_{872}, \beta_{873}, \beta_{874}, \beta_{875}, \beta_{876}, \beta_{877}, \beta_{878}, \beta_{879}, \beta_{880}, \beta_{881}, \beta_{882}, \beta_{883}, \beta_{884}, \beta_{885}, \beta_{886}, \beta_{887}, \beta_{888}, \beta_{889}, \beta_{890}, \beta_{891}, \beta_{892}, \beta_{893}, \beta_{894}, \beta_{895}, \beta_{896}, \beta_{897}, \beta_{898}, \beta_{899}, \beta_{900}, \beta_{901}, \beta_{902}, \beta_{903}, \beta_{904}, \beta_{905}, \beta_{906}, \beta_{907}, \beta_{908}, \beta_{909}, \beta_{910}, \beta_{911}, \beta_{912}, \beta_{913}, \beta_{914}, \beta_{915}, \beta_{916}, \beta_{917}, \beta_{918}, \beta_{919}, \beta_{920}, \beta_{921}, \beta_{922}, \beta_{923}, \beta_{924}, \beta_{925}, \beta_{926}, \beta_{927}, \beta_{928}, \beta_{929}, \beta_{930}, \beta_{931}, \beta_{932}, \beta_{933}, \beta_{934}, \beta_{935}, \beta_{936}, \beta_{937}, \beta_{938}, \beta_{939}, \beta_{940}, \beta_{941}, \beta_{942}, \beta_{943}, \beta_{944}, \beta_{945}, \beta_{946}, \beta_{947}, \beta_{948}, \beta_{949}, \beta_{950}, \beta_{951}, \beta_{952}, \beta_{953}, \beta_{954}, \beta_{955}, \beta_{956}, \beta_{957}, \beta_{958}, \beta_{959}, \beta_{960}, \beta_{961}, \beta_{962}, \beta_{963}, \beta_{964}, \beta_{965}, \beta_{966}, \beta_{967}, \beta_{968}, \beta_{969}, \beta_{970}, \beta_{971}, \beta_{972}, \beta_{973}, \beta_{974}, \beta_{975}, \beta_{976}, \beta_{977}, \beta_{978}, \beta_{979}, \beta_{980}, \beta_{981}, \beta_{982}, \beta_{983}, \beta_{984}, \beta_{985}, \beta_{986}, \beta_{987}, \beta_{988}, \beta_{989}, \beta_{990}, \beta_{991}, \beta_{992}, \beta_{993}, \beta_{994}, \beta_{995}, \beta_{996}, \beta_{997}, \beta_{998}, \beta_{999}, \beta_{1000}$

Machine Learning algorithms:

- Python packages: random forest in the sklearn.

- Five (5) supervised Machine Learning (SML) techniques used were: Support Vector (KNN), Classification and Regression Tree (Decision Tree) (CART), Naive Bayes (NB), Stochastic Gradient Boosting (GB), and Adaptive Boosting (AB).

- The model predictions were evaluated by performance using the following metrics: (i) Fold-Cross-Validation Accuracy (CVA) and Prediction Accuracy (PA).

$$PA = \frac{TP + TN}{TP + FP + FN + TN}$$

where TP = True Positive and FN = False Negative

### Monte-Carlo Simulation

- Python packages: pandas-monte-carlo PyPI was used to generate the simulated data.
- Parameters (simulations = 20, burn-in goal = 0.5).

## Results

### Monte-Carlo Simulation (MCS):

Figure 3 below shows the simulated data made by MCS against the observed data for all the factors that affect the decisions of individuals during an emergency evacuation.

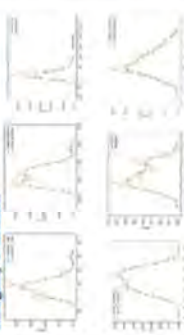


Figure 3 Density plots of the simulated and the observed datasets representative for each independent variable.

Supervised Machine Learning (SML):

Figure 4 left shows the performance of SML models based on the 10-fold cross-validation and Prediction Accuracy for ecological and judgment data respectively. 80% of the data is used to train the model and 20% of the data is used to test the model.

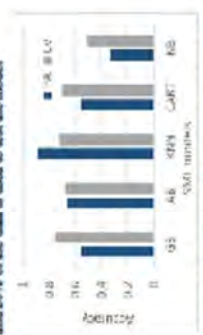


Figure 4 Performance of SML models based on CVA and PA prediction accuracy for the Ecology data.



Figure 5 Performance of SML models based on CVA and PA prediction accuracy for the Judgment data.

## Results

### Lens Model Parameters

TABLE 1: Performance of models based on Lens-model parameters,  $\alpha = 0.66$

Dist	G	C	R <sub>1</sub>	R <sub>2</sub>
AB	0.258	0.377	0.316	0.745
GB	0.447	0.378	0.316	0.745
KNN	0.655	0.143	0.661	0.654
CART	0.6	0.378	0.316	0.745
NB	0.447	0.293	0.25	0.745

## Conclusion

### Monte-Carlo Simulation:

- The LM model parameter  $\alpha$  describes the relationship made by the judgement on measured 0.66 indicating that MCS simulated the judgement data with 66% accuracy.

### Machine Learning algorithms:

- The five non-linear SML algorithms were used within the LM to capture the non-linear strategies in the criterion. A common problem after using the traditional logistic regression model.
- Regarding modeling the ecology (left side of the 7x5 KNN map) using the other SML models in response to data for criterion ecological velocity. On the right side of the LM, human judgments, all SML models apply proved to be best model.
- The relatively low CVA values across all the SML models indicate that the models were able to capture the non-linear strategies that exist in the LM.

- Overall, this study contributes to disaster management literature by providing data-supported models to guide decision making when there is limited information.

### Acknowledgement

The authors would like to thank Center for Advanced Transportation Mobility, for financially supporting this research under grant No. 69A355147125 and also North Carolina A&T State University for providing the infrastructure respectively.

# Transportation Network Resilience in Charlotte, North Carolina for Day-to-Day Disruptions



David Richmond, Xiuli Qu

North Carolina Agricultural and Technical State University, Greensboro, NC-27411



## Introduction

Roads are vulnerable to day-to-day disruptions such as weather conditions, human errors, and/or technological failures. Disruptions can have such effects on the transportation network, such as the cause of delays and damage to major infrastructure. Charlotte, NC, is a major city, ranking the 16<sup>th</sup> most populous city in the United States. Being such a large city, it is the hub of major businesses, travel, and events, which often mean that there is a high utilization of its road network on a daily basis. For this reason, the objective of this study is to analyze the network connectivity and topology of Charlotte, NC. In order to quantify the resilience of the overall network and to identify the routes that are the most critical to the efficiency of the transportation network with respect to daily disruptions.



Fig. 1: Transportation Network of Charlotte

## Background

- Resilience analysis is used in order to quantify the ability of a network to absorb and react to unexpected events.
- Resilience identifies links in the network that, if a disruption were to occur, could have devastating effects on the overall network.
- The majority of approaches are purely topological and/or based on static network connectivity analysis.
- Betweenness centrality (BC) has been widely utilized to assess road resilience by identifying topologically vulnerable links and intersections.

## Methodology

**Defining Transportation Network**  
Let  $G(V, E)$  be a subset of the transportation network of Charlotte, where  $V = \{v_1, v_2, \dots, v_n\}$ ,  $E = \{e_1, e_2, \dots, e_m\}$ . Let  $w_i$  be a weight attribute of link  $i$ , such as the distance, where  $w_i > 0, \forall i$ .

**Betweenness Centrality (BC) Algorithm**  
Given a transportation network, the weighted BC algorithm computes the betweenness centrality for each road segment within the network using the following formula:

$$G_B(v) = \sum_{s \in S, t \in T} \frac{\sigma(s, v, t)}{\sigma(s, t)}$$

Let  $S = \{s_1, s_2, \dots, s_k\}$ ,  $T = \{t_1, t_2, \dots, t_l\}$  is a V-A path is defined from  $s \in S$  to  $t \in T$ . Then  $\sigma(s, t)$  is the number of shortest  $s, t$ -paths, and  $\sigma(s, v, t)$  is the number of those paths passing through edge  $e$ . The length of a path is then the sum of weights of the links.



Fig. 2: Transportation network example

## Data Collection and Processing



## Results

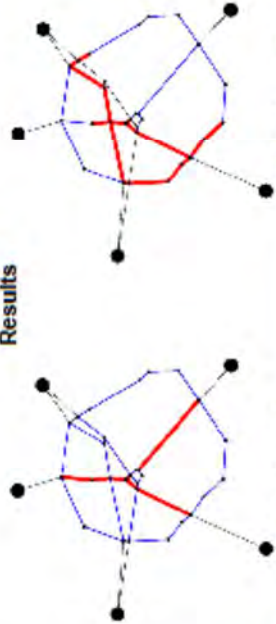


Fig. 3: Critical nodes (BC)

Fig. 4: Critical links (AADT)

## Discussion of Results

- Based on the distance of the road segments, Interstate 77 is a critical route as well as part of Interstate 285 and US highway 74.
- Based on road criticality on the average annual daily traffic, we found that Interstate 85 along with segments of Interstates 485 and 77 are the most critical routes to the transportation system.
- After analyzing the results, we noticed that when AADT is the indicator, only Interstates are considered critical road segments. We infer that this is due to the Interstates having more road capacity than the US-highways. In other words, the higher the road capacity the more volume of traffic.

## Conclusions and Contributions

- We applied the weighted betweenness centrality (BC) algorithm in order to identify road segments that are critical to the resiliency of Charlotte's Transportation system.
- This study examines the Interstates and US-highways in the Charlotte area.
- We also consider the average annual daily traffic (AADT) for 2019 as an indicator.
- Our results can be used to determine which road segments are the most critical to be protected and restored in the event of a day-to-day disruption based on their criticality.

## Future Research

- To have a more accurate model, we will expand the scope of the transportation area by including state routes, as well as primary and secondary roads.
- We will define a directed transportation network model based on the flow of traffic so that our model and result could be more accurate and valid.
- We will also consider other indicators of road criticality such as the average time traveled for each route.

**Acknowledgement**  
David Richmond is supported by the Title II HBCU Fellowship. This project was funded by the Center for Advanced Transportation Mobility (CATM) at NCAT (I-85/77/285), which is one of the DOT Title II University Transportation Centers.



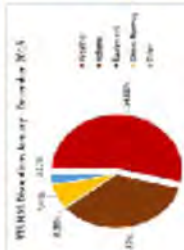
# Prediction of the affected number of passengers during Hurricane Matthew 2016

Harshitha Meda (Ph.D. Candidate)

Advisor : Dr. Lauren B. Davis, Co-Advisor : Dr. Chrysafis Vogiatzis



## Introduction



- Analysis of airlines and airports big data is crucial to recommend appropriate actions during a hurricane disruption.

## Objectives

- To estimate the change in outgoing and incoming airport connections before, during, and after the hurricane.
- To identify the most impacted airlines and understand the influence of their network structure models on this impact during a hurricane disruption.
- To estimate the possible number of passengers that might have been affected during a hurricane.

## Data

- Hurricane Matthew 2016 data from September 1, 2016 to October 31, 2016 was used.
- This data consisted of 117,844 rows and 18 columns of information of four major airports.

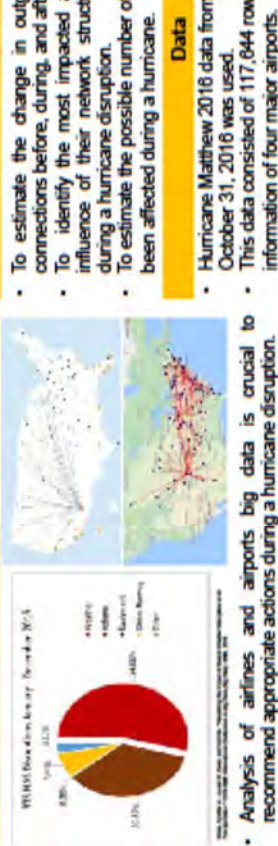
## Conclusions

- The Orlando International airport (MCO) was found to be the most affected airport.
- Southwest airlines was the most affected carrier airline.
- It took almost two days for Southwest airlines to recover from Hurricane Matthew 2016 weather disruption.
- Southwest airlines follows a rolling hub model unlike traditional network structure models.
- Future work is to analyze the role of different carrier airlines network topologies in a hurricane affected area.

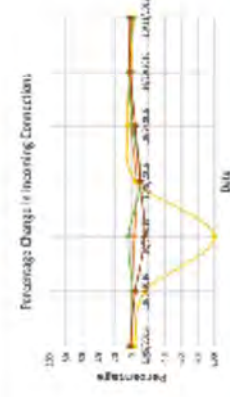
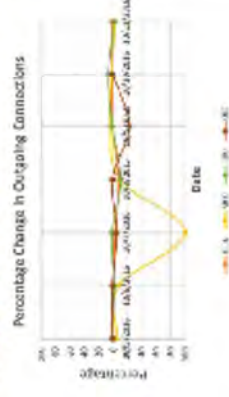
## Acknowledgment

This project is funded by North Carolina Agricultural and Technical State University's Center for Advanced Transportation Mobility, Award #RAC051741725.

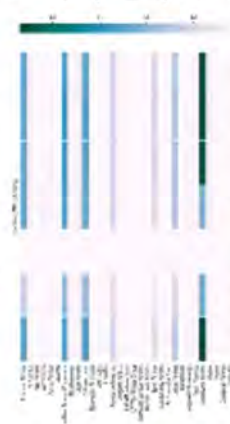
## Results



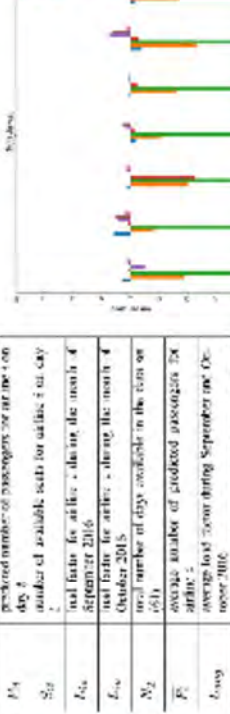
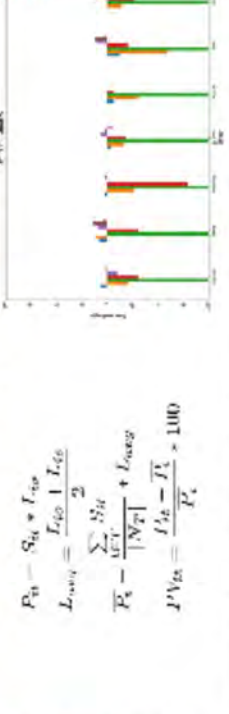
### I. Percentage change in number of incoming and outgoing connections



### II. Most affected departing and arriving airlines



### III. The Predicted number of passengers for the seven affected airlines



Day	$P_{10}$	$S_{10}$	$I_{10}$	$L_{10}$	$N_{10}$	$P_{10}$	$L_{10}$	$P_{10}$
predicted number of passengers for an airline on day $t$								
number of available seats for airline $i$ on day $t$								
total factor for airline $i$ during the month of September 2016								
total factor for airline $i$ during the month of October 2016								
total number of days available in the month of 2016								
average number of predicted passengers for airline $i$								
average total factor during September and October 2016								
percentage change between $P_{10}$ and $P_{10}$ for airline $i$ on day $t$								

$$P_{10} = S_{10} + I_{10}$$

$$L_{10} = \frac{I_{10} + I_{10}}{2}$$

$$P_{10} = \frac{\sum N_{10}}{|N_{10}|} + L_{10}$$

$$P_{10} = \frac{I_{10} - P_{10}}{P_{10}} \times 100$$

# Traffic Analysis During Hurricane Irma Evacuation



Center for Advanced Transportation Mobility (CATM)

Theanna Drennon, Sachin Mhatre, Xiuli Qu, North Carolina A&T State University, Greensboro, NC-27411



## Introduction

Hurricane Irma was the deadliest, costliest cyclone of 2017. Hurricane Irma strengthened into a category 5 storm moved over Cape Verde, Leeward Island, Greater Antilles, Turks and Caicos Islands, The Bahamas, and impacted the U.S. southeast coast. The storm caused 7 million evacuations throughout the impacted areas due to severe flooding and strong winds. The objective of this study was to investigate the evacuation of Hurricane Irma in the impacted areas and the effectiveness of their evacuation preparation and response activities.

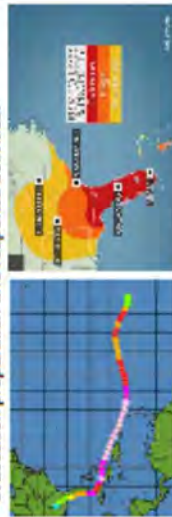


Fig. 1 Track of Hurricane Irma

## Hurricane Irma Evacuation

- At 07:59 Eastern time on September 10th Irma hit the United States with a wind gust of 93 mph in Florida.
- At least 134 deaths, 92 in the United States
- Nearly 6.9 Million left without power in Florida, Georgia, North Carolina, South Carolina, and Alabama
- Evacuation orders were issued to 39 counties in Florida, 24 mandatory and 15 voluntary ones.
- Nearly 7 million people evacuated their homes.
- Allowed to use the left shoulder as a lane for moving traffic on northbound Interstate 75 from Wildwood
- Suspended tolls on all toll roads in Florida
- Before the storm many gas stations in the Gainesville and Miami-Fort Lauderdale areas were out of fuel.
- Gas was 53 cents higher, making each gallon \$2.73.

## Traffic Data

- Time Period: September 8 to September 16
- Location: Marion County (North and South) Suwannee County (East and West)



Fig. 3 Marion County

### Marion (North)



Fig. 4 Suwannee County

### Marion (South)



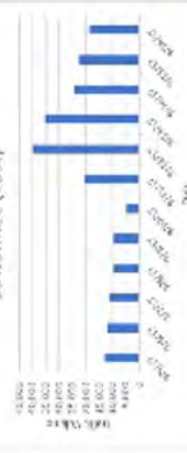
## Conclusions

- High northbound traffic volumes and low southbound volumes from September 6<sup>th</sup> to 9<sup>th</sup>
- High southbound traffic volumes starting on September 11<sup>th</sup>
- Low eastbound traffic volumes and high westbound volumes from September 5<sup>th</sup> to 10<sup>th</sup>
- This is all due to the effect of Hurricane Irma evacuation.
- The flow of traffic coming from Florida spiked as more evacuations were mandated.

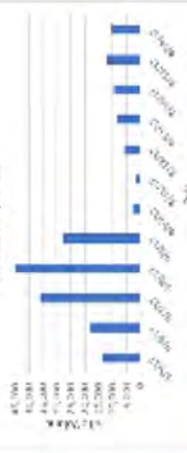
## Acknowledgement

This research was supported by the Center for Advanced Transportation Mobility (CATM), USDOT grant # 69A3551747125.

### Suwannee (East)



### Suwannee (West)





# Traffic Analysis During Hurricane Florence Evacuation

Morgan Lipkins, Sachin Mhatre, Xiuli Qu, North Carolina A&T State University, Greensboro, NC-27411



## Introduction

Due to its catastrophic damage, Hurricane Florence (2018) is still the wettest tropical cycle on record in the Carolinas. Over the course of 19 days from August 31, 2018 to September 18, 2018, Hurricane Florence strengthened to a Category 4 hurricane that moved through Cape Verde, Bermuda and central Atlantic, and made landfall as a Category 1 hurricane in the east coast of the United States. Hurricane Florence resulted in more than 18 evacuation orders and caused devastating flooding across the southeastern United States. The objective of this research study is to investigate the evacuation of Hurricane Florence in the affected areas and the effectiveness of their evacuation preparation and response activities.



Fig. 1 Track of Hurricane Florence

## Hurricane Florence Evacuation

- At 7:15 am EDT September 14<sup>th</sup> Hurricane Florence made landfall in the south of Wrightsville Beach, NC as a Category 1 hurricane with sustained winds of 90 mph
- More Than 1 Million people ordered to evacuate as Hurricane Florence approached on 9/11/18
- More than 18 evacuation orders, with at least 10 mandatory and 7 voluntary evacuations
- Hurricane Florence resulted in 59 direct deaths and was also associated with 30 indirect fatalities.
- Caused up to \$24.23 billion damage

## Traffic Data

- Time Period: September 1 to September 22
- Location: Wake County (East and West)  
Wayne County (East and West)  
Johnston County (East and West)



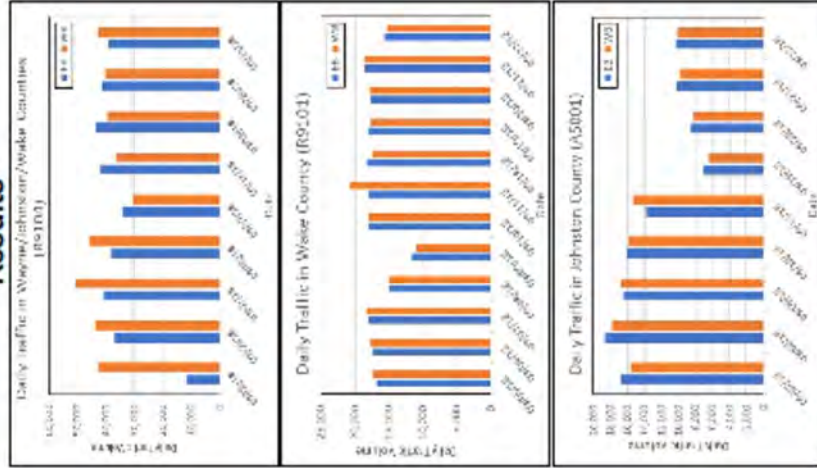
## Observations and Conclusions

- Significantly higher total traffic volumes from 9/7/18 to 9/11/18 than those from 9/19/18 to 9/22/18 in Johnston county (A50001)
- More westbound traffic volumes from 9/5/18 to 9/8/18 than eastbound traffic volumes at the adjacent area of Johnston, Wake and Wayne counties (R9104)
- Sudden decrease in overall traffic volumes on 9/8/18 and 9/9/18 compared to the overall traffic volumes on the other days in Wake county (R9101)
- The change of traffic volumes over time during a hurricane evacuation depends on the location and the topology of the road transportation network.
- The flow of traffic spiked as more evacuations were mandated.

## Acknowledgement

This research was supported by the Center for Advanced Transportation Mobility (CATM), USDOT grant #69A3551747125.

## Results





NORTH CAROLINA AGRICULTURAL  
AND TECHNICAL STATE UNIVERSITY

---

***ANALYSIS OF HURRICANE MATTHEW 2016 DATA TO  
IDENTIFY AIRLINE PASSENGERS DISRUPTION***

---

Harshitha Meda (Ph.D. Candidate)  
Advisor: Dr. Lauren B. Davis  
Co-advisor: Dr. Chrysafis Vogiatzis

**Industrial and Systems Engineering**

AGGIES **DO**

1



NORTH CAROLINA AGRICULTURAL  
AND TECHNICAL STATE UNIVERSITY

---

**Outline**

- Introduction
- Data
- Results
- Conclusions
- Future Work

AGGIES **DO**

2

 NORTH CAROLINA AGRICULTURAL  
AND TECHNICAL STATE UNIVERSITY

---

## Introduction



**AGGIES DO** 003-476 9

3

 NORTH CAROLINA AGRICULTURAL  
AND TECHNICAL STATE UNIVERSITY

---

## Research Objectives

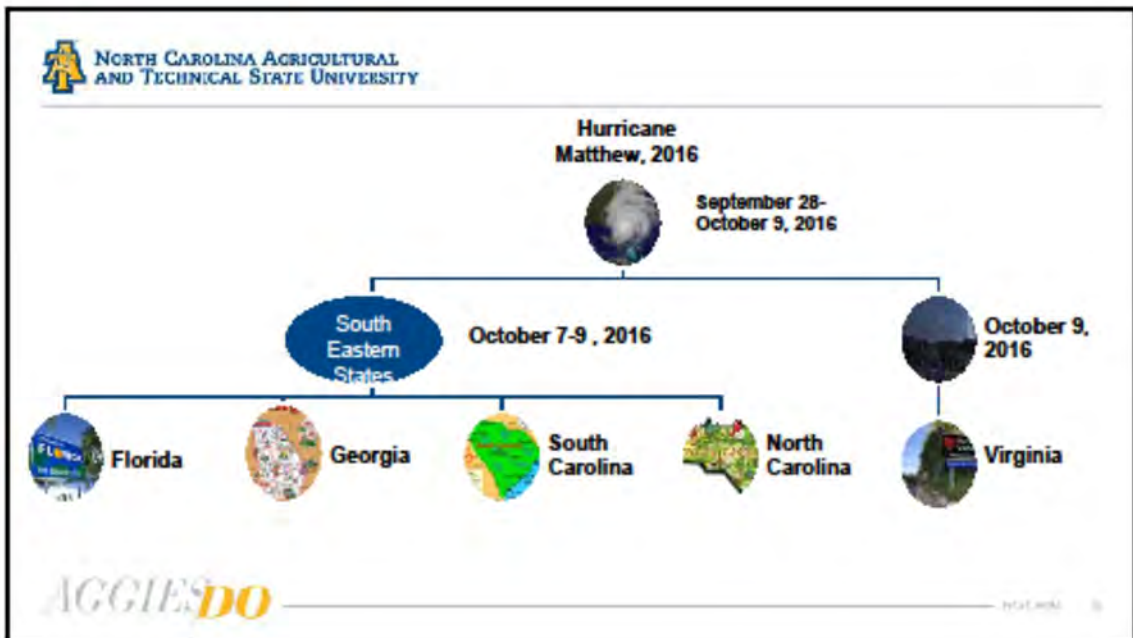
- To identify the affected airports
  - To visualize the outgoing and incoming connections at these airports
- To identify the most impacted airlines
  - To understand the influence of their network structure
- To estimate the percentage of affected passengers

**AGGIES DO** 003-476 9

4



5



6

**North Carolina Agricultural and Technical State University**

## Data

Data  
117,644 rows  
18 columns

- September 1, 2016 to October 31, 2016
- Orlando International Airport
- Raleigh-Durham International Airport
- Ronald Reagan Washington National Airport
- Norfolk International Airport

**AGGIES DO**

7

**North Carolina Agricultural and Technical State University**

## Data



Data Wrangling



October 5-11, 2016



Python (Pandas, Networkx),  
Microsoft Excel

**AGGIES DO**

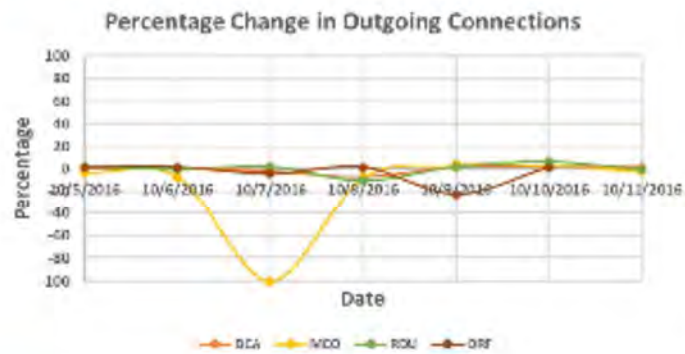
8

## Objective 1

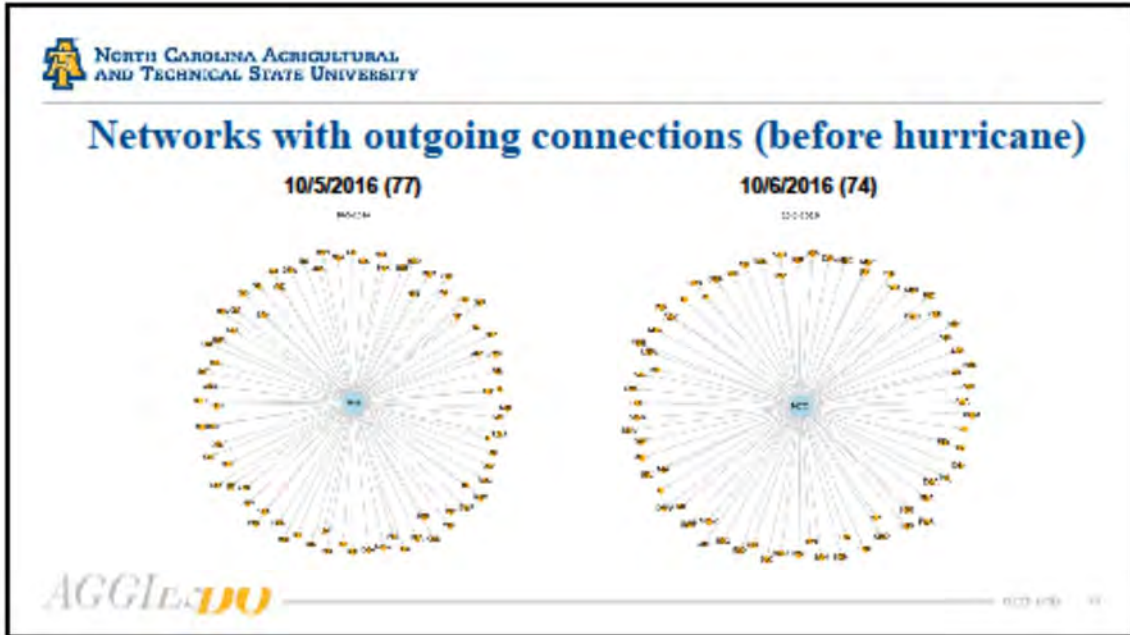
- To identify the affected airports
  - To visualize the outgoing and incoming connections at these airports

9

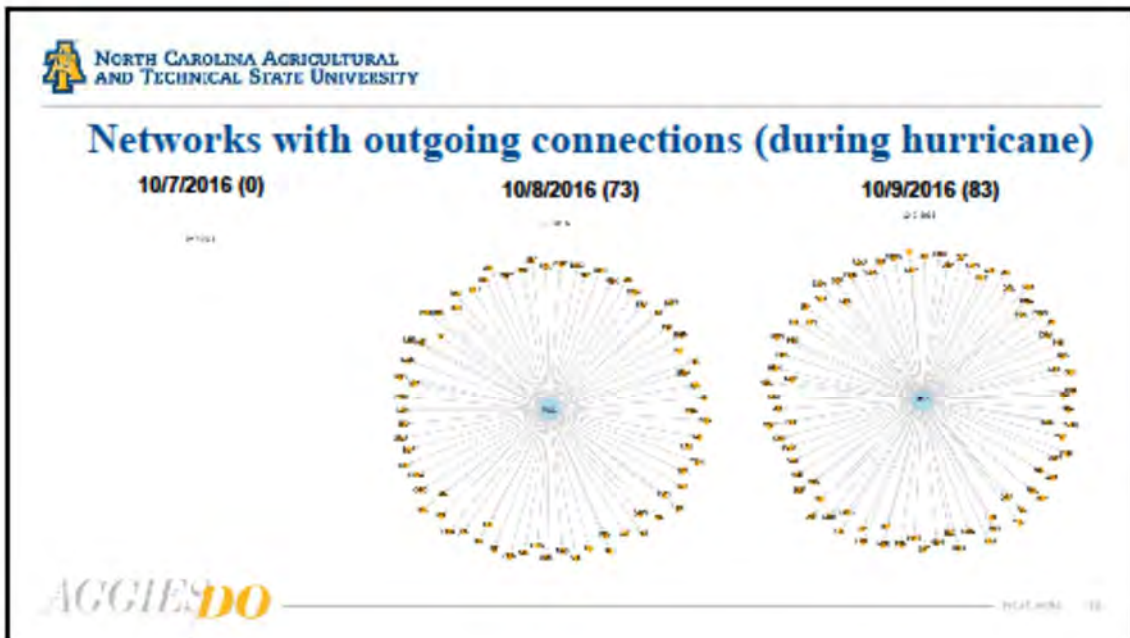
## Outgoing connections at four major airports



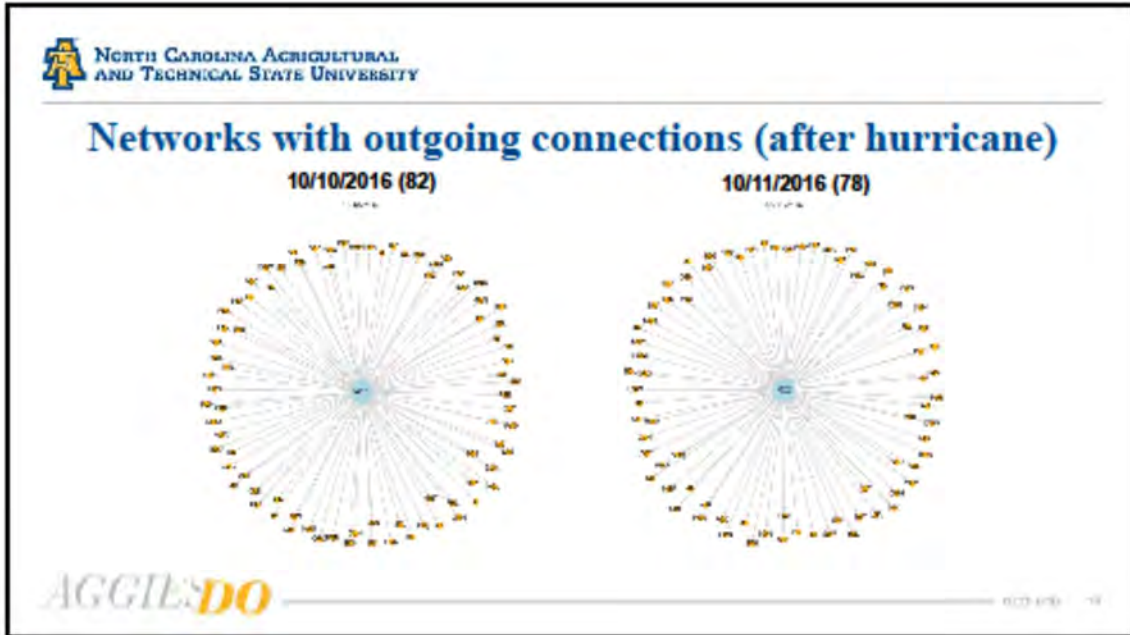
10



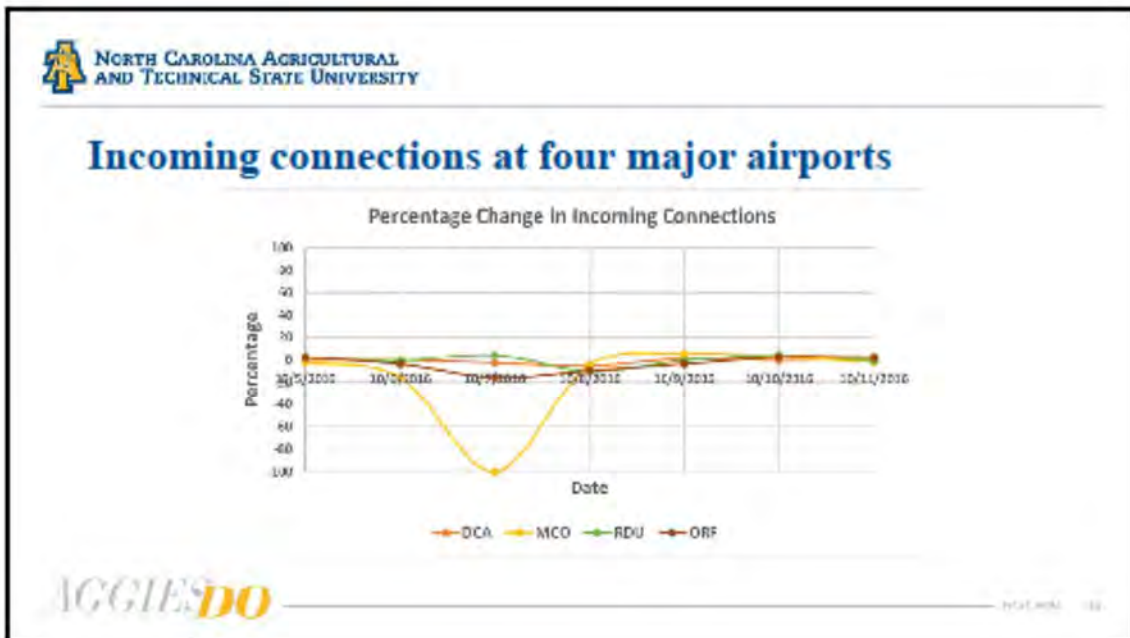
11



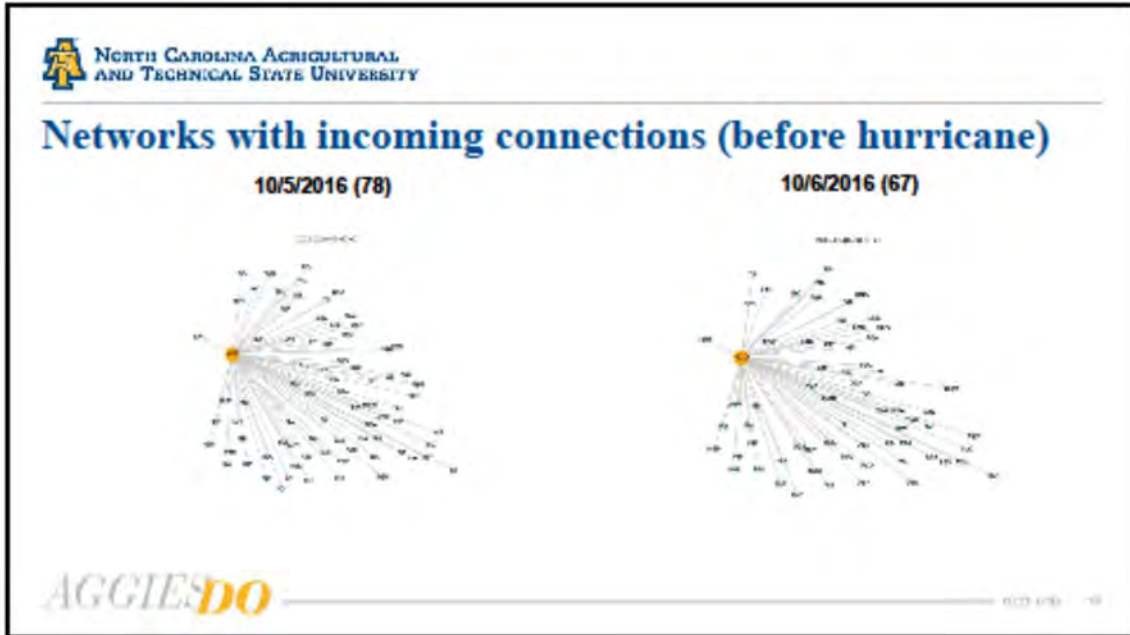
12



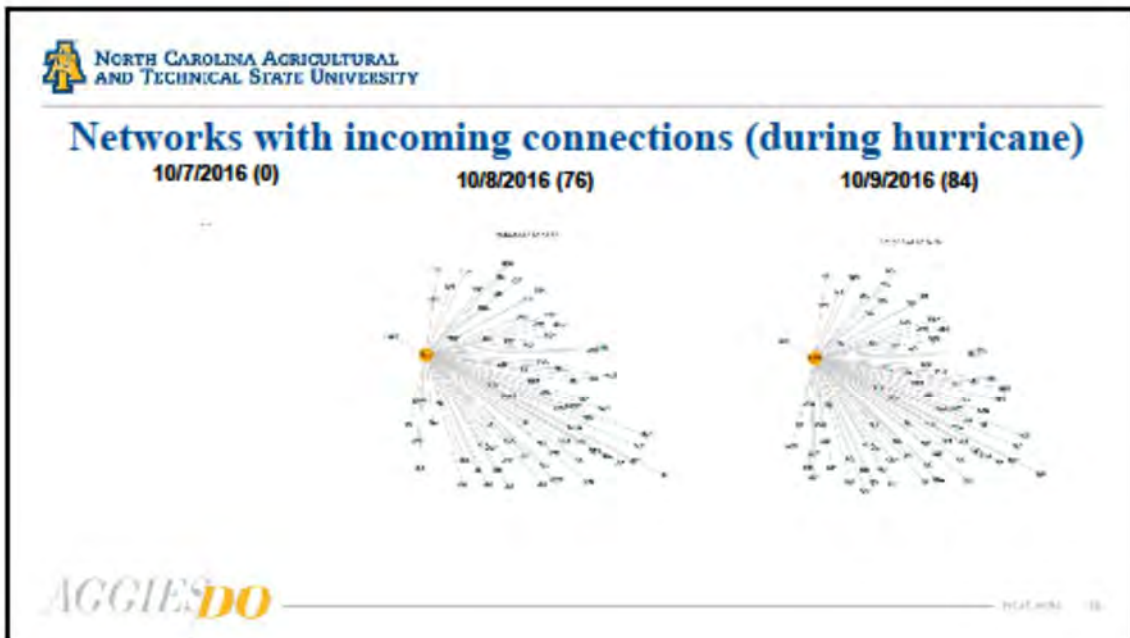
13



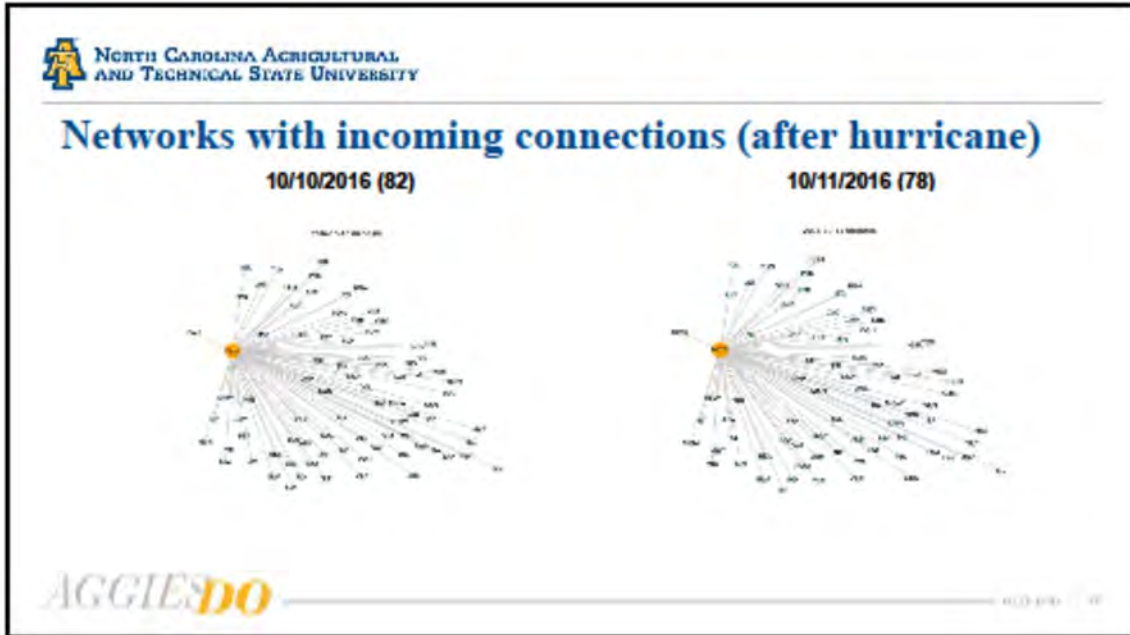
14



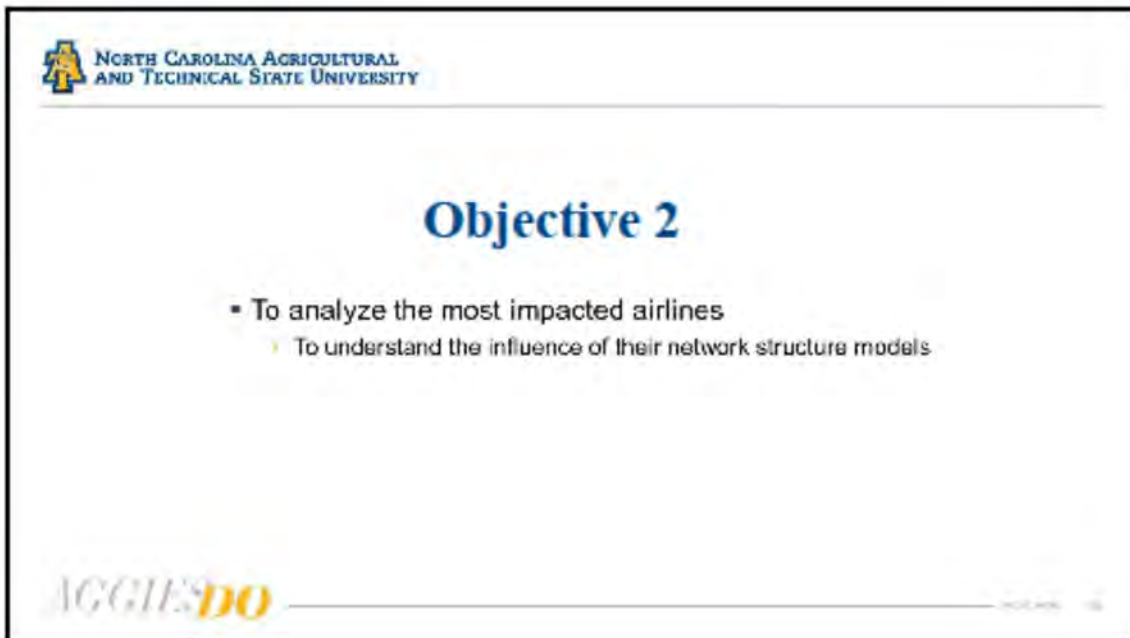
15



16



17



NORTH CAROLINA AGRICULTURAL AND TECHNICAL STATE UNIVERSITY

## Objective 2

- To analyze the most impacted airlines
  - To understand the influence of their network structure models

AGGIES DO

18



19

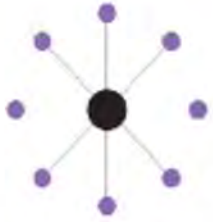


20

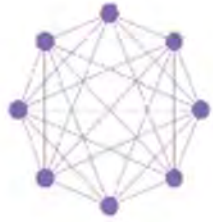

**NORTH CAROLINA AGRICULTURAL AND TECHNICAL STATE UNIVERSITY**

---

## Network Structure models in airlines



**Hub**  
*linking 9 points, requires 8 routes*



**Point-to-Point**  
*linking 8 points, requires 28 routes*


© 2014

21


**NORTH CAROLINA AGRICULTURAL AND TECHNICAL STATE UNIVERSITY**

---

## Role of MCO for affected airlines and their network structure model

Airline Service Name	Role of MCO	Model
American Airlines	N/A	Hub spoke model (ten hubs)
Frontier	Focus City	Hub spoke model with 10 focus cities and 1 hub
JetBlue	Focus City	Focus city model(6 focus cities)
Spirit	Focus City	Point to Point model
Southwest	Focus City	Point to point with rolling hub model (8 focus cities and 11 operating bases)
United	N/A	Hub Spoke model (eight hubs)
Delta	N/A	Hub Spoke model(9 hubs and 2 focus cities)


© 2014

22

## Objective 3

- To estimate the percentage of affected passengers

## Methodology to estimate percent of affected passengers at the MCO

- Analysis is done utilizing the number of available seats present in the data set
- Load factors for September and October 2016 are retrieved from Bureau of Transportation Statistics

$$\text{Load Factor} = \frac{\text{Revenue Passenger miles}}{\text{Available Seats miles}}$$

- Number of miles are assumed to be constant for this study



## Methodology cont.

$$P_{ij} = L_{io} * S_{ij}$$

- $P_{ij}$  is predicted number of passengers for an airline  $i$  on day  $j$  during October month in 2016
- $L_{io}$  is the load factor for an airline  $i$  during October month in the year 2016
- $S_{ij}$  is number of available seats for an airline  $i$  on day  $j$

$$L_{avg} = \frac{(L_{is} + L_{io})}{2}$$

- $L_{is}$  is the load factor for an airline  $i$  during September month in the year 2016
- $L_{avg}$  is the average load factor for an airline during September and October months in the year 2016



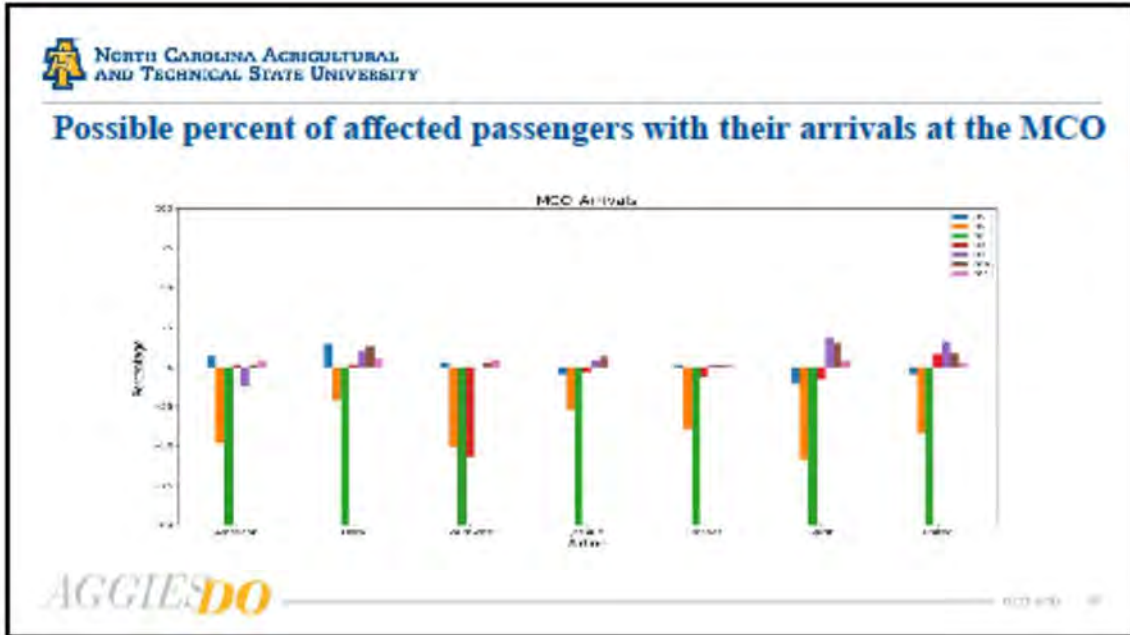
## Methodology cont.

$$\bar{P}_i = \frac{\sum_{t=1}^T S_{it}}{N_T} * L_{avg}$$

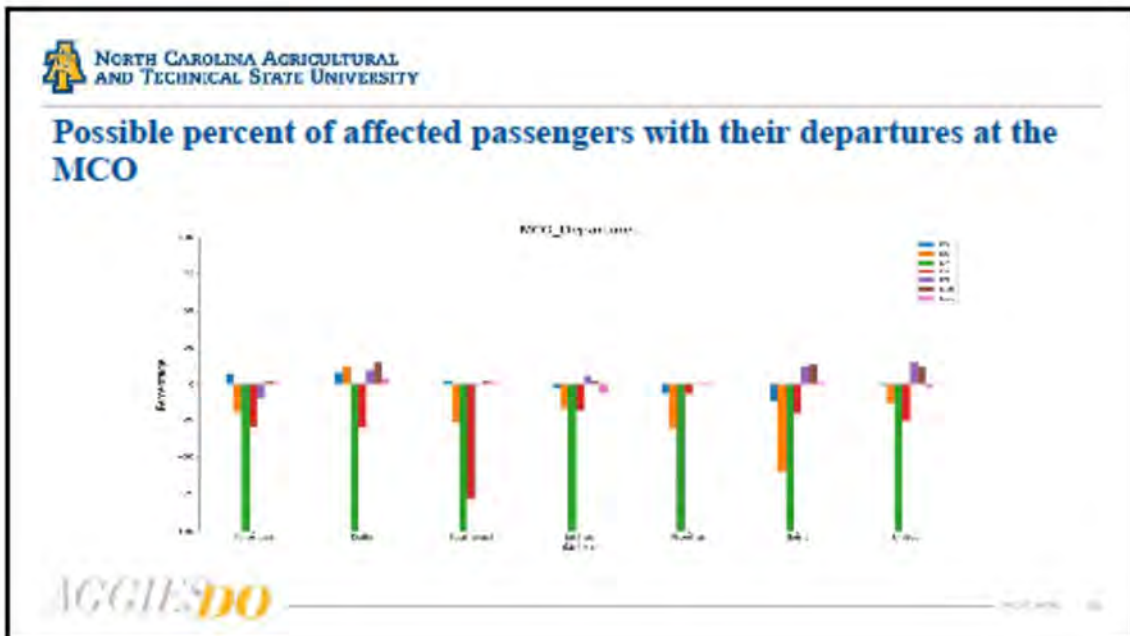
- $\bar{P}_i$  is average number of passengers for an airline  $i$
- $\sum_{t=1}^T S_{it}$  is total number of available seats for an airline  $i$  for a total of  $T$  days i.e. 81
- $N_T$  is the total number of days available in the data set

$$PV_{ij} = \frac{(P_{ij} - \bar{P}_i)}{\bar{P}_i} * 100$$

- $PV_{ij}$  is the percentage of the predicted number of affected passengers for an airline  $i$  on day  $j$



27



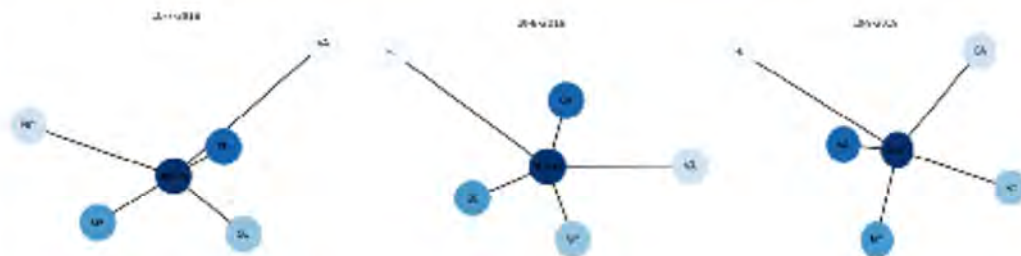
28

## Conclusions

- This study presents a data-driven approach
  - To identify the impacted airlines
  - To predict the affected number of passengers using network theory related concepts
- Southwest Airlines is the most affected carrier airline
- Orlando International Airport is the most affected airport
- This work could be relevant to apply to either a regional or international airports
- This approach could be applied to any kind of weather or human-made disruption at different airports

29

## Storm distances on hurricane occurring days



30



## Future Work

- Future work would be
  - To extend this analysis to other major airports present in the data
  - Based on the hurricane dates
- Other possible work would be to analyze
  - The role of different carrier airlines network topologies in hurricane affected areas.

31



## Thank you



32



NORTH CAROLINA AGRICULTURAL  
AND TECHNICAL STATE UNIVERSITY



EMBRY-RIDDLE  
AERONAUTICAL UNIVERSITY

---

***TRAFFIC PATTERN DISCOVERY DURING  
RECENT HURRICANE EVACUATIONS  
IN NORTH CAROLINA : A CASE STUDY***

---

Sachin Mhatre  
Graduate student at NC A & T

Guided by: Dr. Xiuli Qu  
Associate Professor at NC A&T  
7<sup>th</sup> UTC Conference, March. 26-27, 2020



**CATM**  
Center for Advanced Transportation Mobility

1



NORTH CAROLINA AGRICULTURAL  
AND TECHNICAL STATE UNIVERSITY



EMBRY-RIDDLE  
AERONAUTICAL UNIVERSITY

---

**Outline**

- Introduction
- Motivation
- Research Objectives
- Previous Studies
- Data
- Results
- Conclusions



**CATM**  
Center for Advanced Transportation Mobility

7<sup>th</sup> Annual UTC Conference for Southeastern Region

1

2



**NORTH CAROLINA AGRICULTURAL  
AND TECHNICAL STATE UNIVERSITY**



**EMBRY-RIDDLE  
AERONAUTICAL UNIVERSITY**

---

## Introduction

### Overview

- Frequency and intensity of natural disasters increasing
- Effect of natural disasters to critical infrastructure
- Mass evacuation during hurricanes





**CATM**  
Center for Advanced Transportation Metrics

7<sup>th</sup> Annual UTC Conference for Southeastern Region

**2**

3



**NORTH CAROLINA AGRICULTURAL  
AND TECHNICAL STATE UNIVERSITY**



**EMBRY-RIDDLE  
AERONAUTICAL UNIVERSITY**

---

## Motivation

### Hurricane Florence in North Carolina

- Evacuation orders in southeastern North Carolina
- Government agencies response to the incoming hurricane
- Critical preparation plan for mass movement of people





**CATM**  
Center for Advanced Transportation Metrics

7<sup>th</sup> Annual UTC Conference for Southeastern Region

**3**

4



**NORTH CAROLINA AGRICULTURAL  
AND TECHNICAL STATE UNIVERSITY**



**EMBRY-RIDDLE  
AERONAUTICAL UNIVERSITY**

---

## Research Objectives

- To analyze the hourly traffic flow data during hurricane evacuations.
- To discover space-time traffic patterns during hurricane evacuations.
- To investigate the relationship between traffic patterns and factors such as forecasted hurricane path and intensity, evacuation orders, etc.





Center for Advanced Transportation Metrics

7th Annual UTC Conference for Southeastern Region

4

5



**NORTH CAROLINA AGRICULTURAL  
AND TECHNICAL STATE UNIVERSITY**



**EMBRY-RIDDLE  
AERONAUTICAL UNIVERSITY**

---

## Previous Studies

Study/Methodology	Optimization	Simulation	Temporospatial	Empirical
Liu et. al, 2005	✓	✓		
Wolshon, 2008				✓
Wolshon & McArdle, 2009			✓	
Archibald and McNeil, 2012			✓	
Bish & Sherali, 2013	✓			
Sun et al, 2017	✓			



Center for Advanced Transportation Metrics

7th Annual UTC Conference for Southeastern Region

5

6



**NORTH CAROLINA AGRICULTURAL  
AND TECHNICAL STATE UNIVERSITY**



**EMBRY-RIDDLE  
AERONAUTICAL UNIVERSITY**

---

## Data

*Source of the Data*

- North Carolina Department of Transportation
- Traffic Survey Group



**NCDOT Divisions**



Center for Advanced Transportation Metrics

7th Annual UTC Conference for Southeastern Region

**6**

7



**NORTH CAROLINA AGRICULTURAL  
AND TECHNICAL STATE UNIVERSITY**

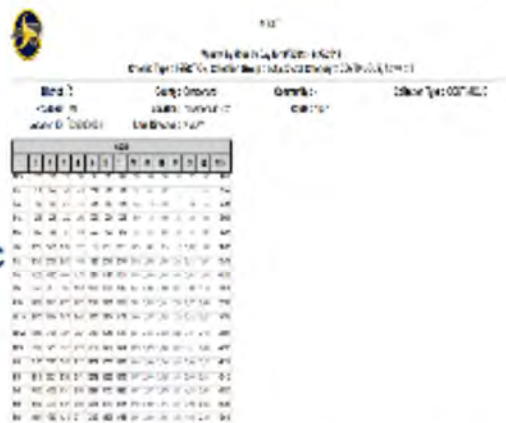


**EMBRY-RIDDLE  
AERONAUTICAL UNIVERSITY**

---

*Description of Data*

- Traffic volume data in North Carolina during a hurricane evacuation
- Time period: 9/5/2018 - 9/20/2018
- Counties (Data): 42 in NC
- 1 or more sensors for each county in NC
- Each sensor: Sensor Location County, Route, lane direction



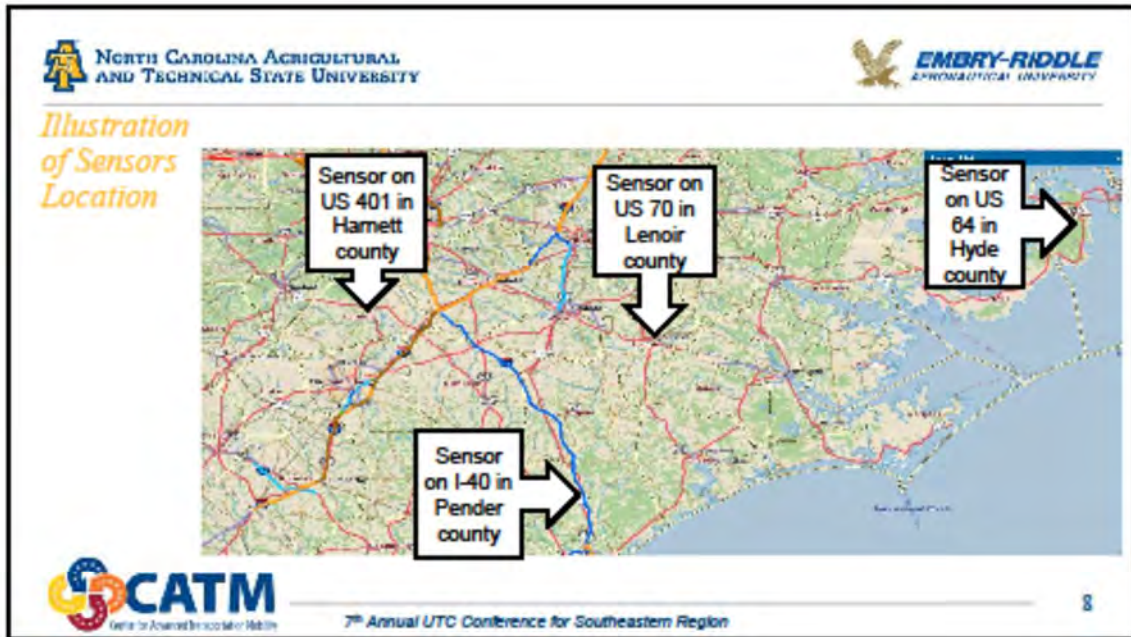


Center for Advanced Transportation Metrics

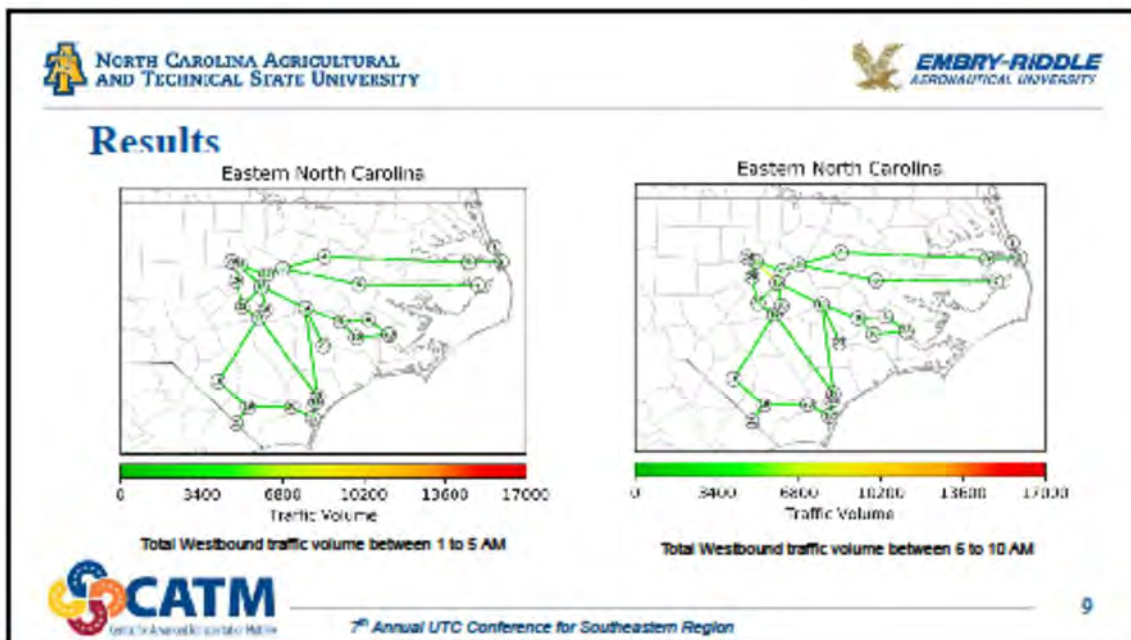
7th Annual UTC Conference for Southeastern Region

**7**

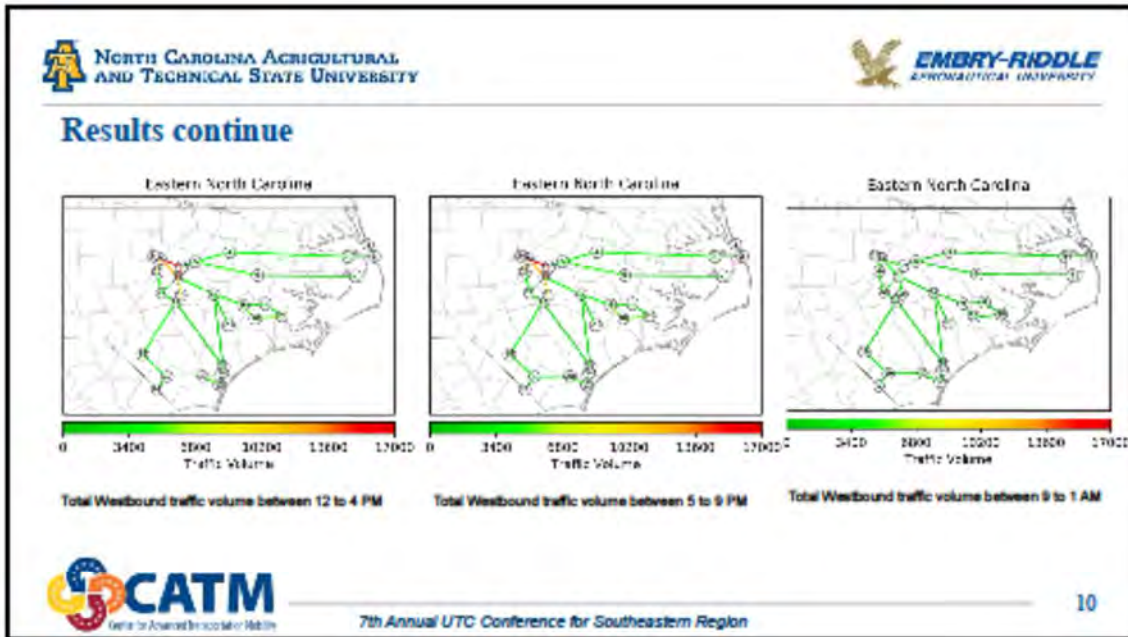
8



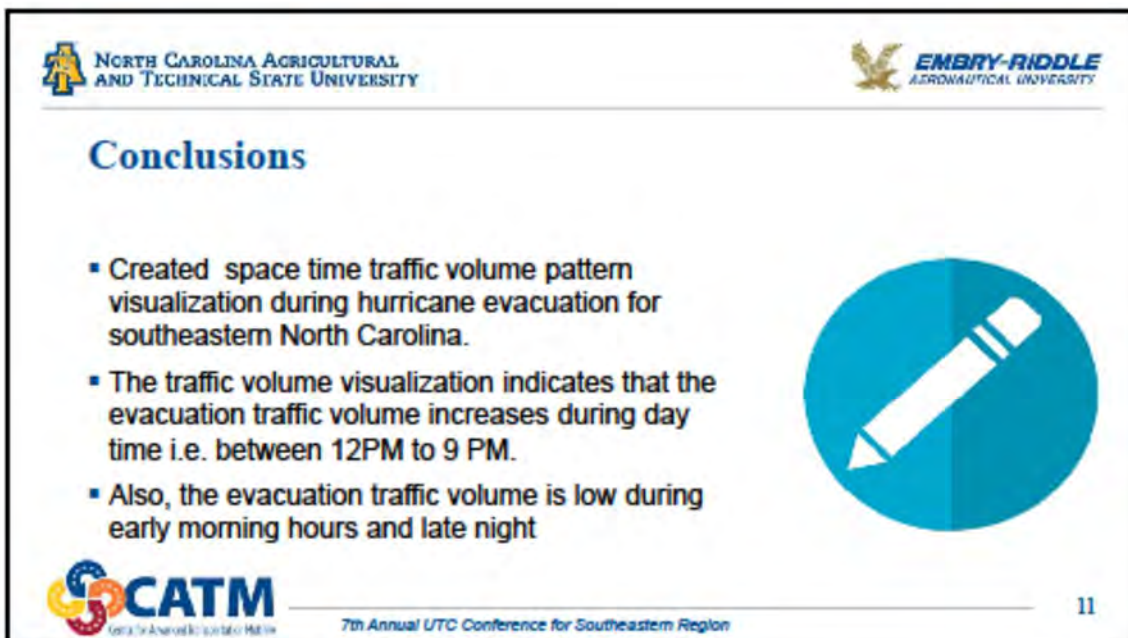
9



10



11



12